УДК: 532.536

CRITICAL AND SUPERCRITICAL PHENOMENA IN BENZENE

© 2019 [1]N.G. Polikhronidi, [1]R.G. Batyrova, [1,2,3]I.M. Abdulagatov*

[1] *Institute of Physics of the Dagestan Scientific Center of the Russian Academy of Sciences, Makhachkala, Dagestan, Russian Federation*
[2] *Geothermal Research Institute of the Russian Academy of Sciences, Makhachkala, Dagestan, Russian Federation*
[3] *Dagestan State University, Makhachkala, Dagestan, Russian Federation*

*ilmutdina@gmail.com

Received: 11.09.2018. Revised: 05.10.2018
Accepted: 05.10.2018

Single- (C_{V_1}) and two-phase (C_{V_2}) isochoric heat capacities, densities (ρ_S), and phase-transition temperatures (T_S) of benzene were measured in the critical and supercritical regions. Measurements were made in the immediate vicinity of the liquid—gas phase transition and the critical point in order to accurately determine the phase transition properties (T_S, ρ_S, C_{V_1} and C_{V_2}). The measurements have been made over the temperature range from 347 to 616 K for 6 liquid and 5 vapor isochores between 265 and 653 kg · m^{-3} at pressures up to 7,5 MPa. The measurements were performed using a high-temperature, high-pressure, nearly constant-volume adiabatic calorimeter. The combined expanded uncertainty of the measurements of density, temperature, and isochoric heat capacity, C_V, at the 95 % confidence level with a coverage factor of $k = 2$ is estimated to be 0,15 %, 15 mK, and 3,0 %, respectively. The measured single- (C_{V_1}) and two-phase (C_{V_2}) isochoric heat capacities along the critical isochore and the saturated liquid (ρ_S') and vapor (ρ_S'') densities near the critical point were used to accurately estimate the theoretically meaningful asymptotic critical amplitudes (A_0^+ and B_0) and related amplitudes for other properties (Γ_0^+, D_0, ξ_0) as well as their universal relations, A_0^+/A_0^-, $A_0^+\Gamma_0^+B_0^2$, $\alpha A_0^+\Gamma_0^+B_0^{-2}$, $D_0\Gamma_0^+B_0^{\delta-1}$, $\xi_0\left(\frac{\alpha A_0^+}{\nu_C}\right)^{1/3}$. Saturated liquid and vapor densities together with measured two-phase C_{v_2} data were used to estimate the values of asymmetric parameters a_3 («complete» scaling parameter) and b_2 of the coexistence curve singular diameter. The experimentally determined asymptotical critical amplitudes A_0^+ and B_0 (fluid-specific parameters) were used to check and confirm the predictive capability of the universal correlation in terms of their dependence on the acentric factor ω, based on C_{v_2} as a function of the specific volume Valong various isotherms were used to calculate second temperature derivatives of the vapor-pressure $\frac{d^2P_S}{dT^2}$ and chemical potential $\frac{d^2\mu}{dT^2}$ and to estimate the value of Yang—Yang anomaly strength parameter R_μ for benzene. The contributions of the vapor-pressure, $C_{VP} = V_C T\frac{d^2P_S}{dT^2}$, and chemical potential, $C_{V\mu} = -T\frac{d^2\mu}{dT^2}$, to the measured total two-phase C_{v_2} were estimated.

K e y w o r d s : adiabatic calorimeter; asymmetryparameter, benzene, critical amplitude; critical point; isochoric heat capacity; Yang—Yang anomaly parameter.

INTRODUCTION

Deep understanding of the properties of near- and supercritical fluids is important from both the fundamental and the technological points of view. Near- and supercritical fluids have a broad range of potential technological applications. A deeper understanding of the microstructure and thermodynamic properties of supercritical fluids will lead to marked improvements in industrial applications of the supercritical technologies for environmental, mechanical, chemical, biological, and geothermal industries. Therefore, new thermodynamic studies of the properties of supercritical fluids are of great importance. For example, it is well-known [1] that supercritical fluids can serve as attractive media for chemical reactions. The physical and transport properties of supercritical fluids lie between those of a gas and those of a liquid and they may provide a tunable reaction medium, in particular for the processes of polymer degradation. Karmore and Madras [2] have studied the degradation of polystyrene in supercritical benzene at 5,0 MPa and found that the degradation rates at supercritical conditions are greatly enhanced as compared to conventional degradation in solution. The study by Karmore and Madras [2] indicates that the degradation rates are significantly enhanced under supercritical conditions of benzene. Fundamental understanding of the polystyrene degradation process in supercritical benzene can considerably minimize the operating costs of the technological processes. Accurate thermodynamic data for near- and supercritical benzene are needed to better understand the microscopic nature of the polystyrene degradation process in supercritical benzene and other fundamental scientific and technological applications.

As part of our continuing efforts to study the critical phenomena in pure fluids [3—7] and binary fluid mixtures [8—11], the isochoric heat capacity measurements have been made for benzene in the critical and supercritical conditions including two-phase and single-phase regions. The measurements were performed using a high-temperature, high-pressure, and nearly constant — volume adiabatic calorimeter. The method and apparatus were successfully used earlier and reported in our previous publications on the accurate measurements of the isochoric heat capacity of pure fluids (light and heavy water, carbon dioxide, *n*-alkanes, alcohols, ionic liquids, etc.) [3—7, 12—15] and of many binary mixtures [8—11, 16, 17] at high temperatures and high pressures. In this work, the same method and apparatus have been employed to measure the two- and single-phase isochoric heat capacities and phase transition properties (T_S , ρ_S', ρ_S'', C_{V_1}, C_{V_2}) of benzene over the temperature range from 347 to 616 K for 6 liquid and 5 vapour isochores between 265 and 642 $kg \cdot m^{-3}$ at pressures up to 7,5 MPa. These temperature and pressure ranges include the critical and supercritical conditions for benzene. Detailed single- and two-phase heat-capacity (C_{V_1} and C_{V_2}) and phase-transition (T_S , ρ_S', ρ_S'') properties measurements near the critical point were used to develop theoretically based scaling-type correlation equations for the heat capacity and the liquid—gas coexistence curve densities based on a «complete» scaling theory of critical phenomena. In this way, very important theoretically meaningful asymptotical critical amplitudes A_0^+ and B_0 and related amplitudes for other properties, such as Γ_0^+, D_0, ξ_0, and their universal relations were accurately determined. The measured two-phase isochoric heat capacity data near the critical point were also used to estimate such theoretically important property as the strength of the Yang—Yang critical anomaly parameter R_μ, which determines the contribution of the vapour-pressure, $C_{VP} = V_C T \dfrac{d^2 P_S}{dT^2}$, and chemical potential, $C_{V_\mu} = -T \dfrac{d^2 \mu}{dT^2}$, heat-capacities to the divergence of experimentally observed total two-phase heat-capacity C_{V_2} near the critical point.

The literature search based on the TRC/NIST archive (TDE search result, http://trc.nist.gov/ thermolit/, ThermoLit) and our own search results revealed that there is only one isochoric heat-capacity source [18] available for benzene in the critical and supercritical regions. Those measurements were made using the same method as in the present work — high-temperature and high-pressure nearly-constant volume adiabatic calorimeter — and covered the temperature range from 300 to 620 K for 30 isochores between 103,9 and 854,7 $kg \cdot m^{-3}$ at pressures up to 70 MPa. However, the quality of the measured C_v values and saturated density data were quite poor (see below). In another work by Chirico and Steele [19] high-temperature two-phase isochoric heat capacities (to within 25 K of T_C) and the critical temperature of benzene were measured by differential-scanning calorimeter (DSC). The measurements were performed in the two-phase region for four constant densities (167,99; 191,69; 359,8 and 411,56 $kg \cdot m^{-3}$) over the temperature range from 310 to 570 K. The measured properties (C_{V_2}, V_S, P_S) were used to determine the saturated heat capacity, C_{sat} as a function of temperature.

The present measurements were focused in the phase-transition and the critical regions in order to accurately determine the phase-transition (T_S, P_S, and ρ_S) and critical (T_C, P_C, and ρ_C) properties. In the present work we studied in detail the critical phenomena in benzene. A total of 1077 saturated liquid and 22 vapor density sources are listed in the NIST Source Data Archive for benzene. Unfortunately, the majority of the reported data for benzene are far from the critical and supercritical regions. All these data were used to compare with the present results to confirm their accuracy and reliability.

Thus, the main objective of the present study was to expand the existing database for benzene to the critical and supercritical regions, i.e., to provide new accurate experimental saturated liquid and vapor density values and isochoric heat capacity data for benzene in the wide temperature and density ranges corresponding to the single- and two-phase regions and the phase transiton curve, including detailed measurements near the critical and supercritical regions. Based on the measured properties (saturated liquid and vapor densities, heat capacity, and other theoretically meaningful parameters), we have calculated a very useful theoretically derived thermodynamic property such as the Yang—Yang anomaly strength parameter, $C_{V\mu} = -T\dfrac{d^2\mu}{dT^2}$, which defines the contribution of the chemical potential ($C_{V\mu}$) to the two-phase singularity of the heat-capacity at the critical point, $C_{V_2} = C_{VP} + C_{V\mu}$. We have also estimated the values of critical amplitudes ($A_0^{\pm}$ and B_0) and their universal ratios, A_0^+/A_0^-, $A_0^+\Gamma_0^+B_0^2$, $\alpha A_0^+\Gamma_0^+B_0^{-2}$, $D_0\Gamma_0^+B_0^{\delta-1}$, $\xi_0\left(\dfrac{\alpha A_0^+}{\nu_C}\right)^{1/3}$, with the amplitudes for other properties (compressibility Γ_0^+, pressure D_0, and correlation radius ξ_0), predicted by the scaling theory of critical phenomena [20—27]. The critical amplitudes of heat capacity (A_0^+) and coexistence curve (B_0) are, in turn, defining other very important theoretically meaningful critical amplitudes, such as $\Gamma_0^+ = 0{,}58B_0^2/\alpha A_0^+$, $D_0 = 1{,}69/\Gamma_0^+B_0^{\delta-1}$, and $\xi_0^+ = 0{,}266(\nu_C/\alpha A_0^+)^{1/3}$ [28] using universal relationships between the critical amplitudes.

Experimentally determined asymptotical critical amplitudes A_0^+, and B_0 (fluid-specific parameters) of benzene were then used to check and confirm the predictive capability of the universal correlation in terms of their dependence on the acentric factor ω based on the corresponding states principle [28]. In addition, we have developed wide-ranging scaling-type correlations for the measured and derived properties of benzene (heat

capacity, saturated densities). All available reported saturated liquid and vapor densities of benzene together with the present measurements were comprehensively evaluated and critically analyzed for their accuracy, reliability and thermodynamic consistency.

EXPERIMENTAL SECTION

Materials

The benzene sample used in this work (CAS # 71-43-2, C_6H_6, product number «ТУ 2631-107-44493179-07», M = 78,114 $g \cdot mol^{-1}$) was supplied by chemical reagents production company joint-stock company EKOS-1 (Moscow, Russia). The supplier furnished its purity assay >0,998 weight fraction, water content was 0,02 mass %. Table 1 lists the commercial sources, purity, water content, and analysis method of the sample used.

Isochoric Heat Capacity, Saturated Liquid and Vapor Density Measurements

The physical basis the method and its theoretical background, the apparatus, the experimental procedures, and the approach to the uncertainty assessment of the measured isochoric heat-capacity (C_V) and the phase-transition properties (T_S, ρ_S', ρ_S'') have been described in detail in our earlier publications [3—17, 29, 30]. In the present work, the same apparatus was employed for isochoric heat capacity measurements of benzene. Only a brief review and the most essential information will be given here. Isochoric heat-capacity ($C_V VT$) measurements were performed with a high-temperature, high-pressure, and nearly constant-volume adiabatic calorimeter [3—17]. The adiabatic conditions were reliably maintained in this calorimeter using a layer of a semiconductor (Cu_2O — a highly sensitive thermo-element) between the thin-walled inner spherical vessel and thick-walled outer spherical vessel. Cuprous oxide (Cu_2O) has a very high thermoelectric power α (about 1150 μV/K) in comparison with other semiconductors. The semiconductor layer (Cu_2O) between the inner and outer vessels is serving as a sensor detecting deviations of the system from adiabatic conditions. This system is detecting extremely small temperature differences (10^{-6} to 10^{-5} K) between the inner and outer calorimetric vessels. The electric field intensity, ε, in the semiconductor layer is proportional to the temperature difference (grad T), i.e., $\varepsilon = \alpha \text{grad}\, T$. The heat that is released by the micro-heater located in the calorimeter (inner vessel) is used only to heat the fluid immersed inside the inner thin-walled vessel of the calorimeter and a thin layer of semiconductor (Cu_2O) that directly adjoins it. Since Cu_2O has a small thermal conductivity ($\lambda \approx 2{,}09$ $W \cdot m^{-1} \cdot K^{-1}$), use of this semiconductor leads to only negligibly small heat losses by conducting and can be readily estimated as $\Delta Q_{los} = \lambda \frac{\Delta T}{d} S\tau$, where λ is the thermal conductivity of cuprous oxide, S is the surface area of the cuprous oxide layer, d is the thickness of the cuprous oxide layer, and ΔT is about 10^{-4} K. The out-of-balance electrical signal from the integrating thermo-element (Cu_2O) is applied

Table 1

Benzene sample description studied in this work (chemical formula C_6H_6, ТУ 2631-107-44493179-07).

Sample	M ($g \cdot mol^{-1}$)	CAS #	Source	Purity	H_2O content
Benzene	78,114	71-43-2	EKOS-1	>0,998 (wt. fraction)	0,02 mass %

first to the input of an amplifying micro-voltmeter whose output feeds a high-precision temperature regulator (HPTR) which is controlling the inner and outer heaters powers. Simultaneously, the layer of semiconductor (Cu_2O) between the inner and outer spheres plays the role of a differentiating medium transmitting pressure to the stronger outer shell and as a highly sensitive thermo-element that can serve as a sensor detecting the deviations from adiabatic conditions or temperature difference between the inner and outer calorimetric spheres. Therefore, this method, in contrast to a vacuum adiabatic calorimeter, allowed to measure the C_V of fluids at high pressures (up to 100 MPa and above) and at high temperatures (up to 1000 K) (see, for example [31]).

In this method, the heat capacity is obtained from the measurements of the mass of the fluidin side the calorimeter, m; the electrical energy released by the inner heater, $\Delta Q = IU\tau$, where U and I are the voltage drop across the heater and the current passing through the heater, respectively; τ is the heating time; the temperature change, ΔT, resulting from addition of an electrical energy ΔQ; and the empty calorimeter heat capacity, C_0. The final working equation for the method is

$$C_V = \frac{1}{m}\left(\frac{\Delta Q}{\Delta T} - C_0\right). \tag{1}$$

The values of the empty calorimeter heat capacity C_0 were determined using a calibration procedure. For this calorimeter, the average value of C_0 is about 190 $J \cdot K^{-1}$, which is much lower ($C_0 \ll mC_V$) than the total heat capacity of the system [calorimeter + sample] (filled calorimeter). The density of the sample at a given temperature T and pressure P was calculated from the simple relation $\rho = m/V_{PT}$, where m is the filling mass of the sample in the calorimeter and

$$V_{PT} = V_{P_0T_0}\left[1 + 3\alpha(T - T_0) + \beta(P - P_0)\right], \tag{2}$$

is the temperature- and pressure-dependent volume of the calorimeter. In Eq. (2), $V_{P_0T_0} = 102{,}51 \pm 0{,}01$ cm^3 is the volume of the calorimeter at a reference temperature $T_0 = 293{,}65$ K and at atmospheric pressure (101 kPa), and α is the thermal expansion coefficient of the calorimeter material (stainless steel 10X18H9T) as a function of temperature [7, 9]. The pressure expansion coefficient of the calorimeter ($\beta = (21{,}2 \pm \pm 2{,}4) \cdot 10^{-4}$ $cm^3 \cdot MPa^{-1}$) was determined experimentally using the method developed in our earlier work [29]. The value of $V_{P_0T_0}$ was measured using the density of a standard fluid (pure water) with well-known PVT values (IAPWS standard, Wagnerand Pruß [32]).

The combined expanded uncertainty of the calorimeter volume V_{PT} at a given temperature and pressure was about 0,05 %. The uncertainty of the sample mass m was estimated to be 0,006 %. The uncertainty of temperature measurements was less than 15 mK. A detailed uncertainty analysis of the method (all of the measured quantities and corrections) is given in our previous publication [33]. The experimental uncertainties of the isochoric heat capacity measurements were evaluated according to recommendations [34, 35] using the working equation (1) and experimental relative uncertainties of all the measured quantities in Eq. (1), including T and ρ measurements, $u(m) = 3 \cdot 10^{-5}$, $u(\Delta T) = 3 \cdot 10^{-3}$, $u(\tau) = 1 \cdot 10^{-4}$, $u(U) = 5 \cdot 10^{-5}$, $u(C_0) = 0{,}02$, $u(\rho) = 1{,}5 \cdot 10^{-1}$. The values of partial derivatives $\left(\partial C_V/\partial T\right)_\rho$ and $\left(\partial C_V/\partial \rho\right)_T$ were estimated from the experimental C_V data. The correction due to non-isochoricity of the heating process (systematic uncertainty), i.e., changes of the system volume, $V_{PT}(T)$, was estimated as

$$C_V = C_V^{\exp} - \left(\frac{\partial P}{\partial T}\right)_V \frac{dV_{PT}}{dT}\frac{T}{m}, \tag{3}$$

where C_V is the corrected heat capacity at constant volume; C_V^{exp} is the experimental value of the heat capacity; V_{PT} is the volume of the calorimeter at given T and P (Eq. 2), which can change slightly with temperature and pressure; m is the mass of the sample. The values of $(\partial P/\partial T)_v$ were measured directly in the present calorimetric experiment using the quasi-static barograms method [36]. The corrections are usually within 1,5—3,0 %, depending on the pressure and temperature ranges. Based on a detailed analysis of all the sources of uncertainties likely to affect the determination of C_V with the present system, the combined expanded ($k = 2$) uncertainty of the heat-capacity measurements, with allowance for the propagation of uncertainty related to the departure from true isochoric conditions of the heating process, is estimated to be 3 %.

The heat capacity was measured as a function of temperature at nearly constant density (quasi-isochores). The calorimeter was filled at room temperature, sealed, and heated along a selected liquid or vapor quasi-isochore. Each run was normally started in the two-phase (L + V) region and completed in the single-phase region, liquid (L) or vapor (V) depending on the filling factor. Between the initial two-phase (L + V) and the final single-phase (L or V) states, the system undergoes a liquid—gas phase transition at temperature T_S for each fixed density ρ (L of V). Therefore, this method enables one to determine the transition temperature T_S as a heat capacity abrupt point (abruptness in the heat-capacity, $\Delta C_V = C_{V_2} - C_{V_1}$, value) and reliable single-(C_{V_1}') and two-phase (C_{V_2}') liquid (′) or single-(C_{V_1}'') and two-phase (C_{V_2}'') vapor (″)heat capacities at saturation for each fixed quasi-isochore (liquid ρ_S' or vapor ρ_S''). Also, the temperature behavior of the heat capacity was monitored using the quasi-static thermogram technique (reading of PRT, $T - \tau$ plot at isochoric heating of the sample). The magnitude of the thermogram slopes,$(dT/d\tau)$, changes before and after the phase transitions are proportional to the heat capacity jump ΔC_V, which diverges at the critical point as $\Delta C_V \propto (T - T_C)^{-\alpha}$ [37, 38]. This makes it easy to detect any types of phase transitions (L—L, L—S, L—V, S—V) occurring in the system near the phase transition points (even for weak phase transitions phenomena) [39—47]. Therefore, at the same calorimetric experiment we can accurately measure isochoric heat capacities in the single-phase (C_{V_1}'-liquid, C_{V_1}''-vapor,) and two-phase regions (C_{V_2}'-liquid, C_{V_2}''-vapor) and the saturation liquid (ρ_S') and vapor (ρ_S'') densitiesat a given temperature T_S. The method was also successfully used for simultaneous measurements of the vapor pressure (P_S), single-phase PVT-properties, and the thermal pressure coefficient (γ_V) by supplying the calorimeter with a calibrated tenso transducer (a piezo-calorimeter; see details in our previous several publications [48—51]).

RESULTS AND DISCUSSION

The measurements of single- and two-phase isochoric heat capacities, C_V, for benzene were made along 6 liquid and 5 vapor isochores between 265 and 653 kg·m^{-3} as a function of temperature from 347 to 616 K at pressures up to 7,5 MPa. Most measurements were made in the immediate vicinity of the phase transition temperatures from two- to single-phase sides for each studied isochores to precisely determine the phase boundary properties (T_S, ρ_S', ρ_S'', C_{V_1}', C_{V_1}'', C_{V_2}', C_{V_2}''). Some selected experimental values of temperature, density, and isochoric heat capacity (single- and two-phase)for benzene are presented in Table 2 and plottedin Figs. 1 to 7 in various projections ($C_V - T$, $C_V - \rho$, $C_{V_1}' - T$, $C_{V_2}' - T$, and $C_{V_2} - V$). Figures 1 and 2 show the temperature dependence of the measured C_V along the various selected near-critical liquid and vapor isochores in the single- and two-phase regions in the immediate vicinity of the phase transition and critical temperatures together with the values calculated from the reference fundamental equation

Table 2

Measured two- and single-phase isochoric heat capacities of benzene

ρ = 336,24 kg/m^3		ρ = 310,36 kg/m^3		ρ = 306,70 kg/m^3		ρ = 300,69 kg/m^3	
T, K	C_V, kJ/kgK	*T*, K	C_V, kJ/kgK	*T*, K	C_V, kJ/kgK	*T*, K	C_V, kJ/kgK
416,43	2,117	357,74	1,928	558,09	3,622	557,93	3,663
416,53	2,118	357,85	1,929	558,18	3,615	558,02	3,733
416,63	2,118	357,96	1,930	558,27	3,615	558,11	3,733
416,74	2,119	358,07	1,931	558,36	3,616	558,20	3,733
416,84	2,120	358,19	1,931	558,45	3,616	558,29	3,780
416,94	2,113	358,30	1,932	558,54	3,617	558,38	3,758
417,05	2,121	358,41	1,933	558,63	3,617	558,47	3,669
417,15	2,121	358,52	1,934	558,72	3,617	558,56	3,745
417,25	2,122	378,80	1,987	558,81	3,685	558,65	3,774
417,36	2,122	378,90	1,988	561,47	4,105	558,73	3,750
479,95	2,456	379,01	1,988	561,56	4,145	560,96	4,075
480,05	2,466	379,23	1,989	561,65	4,253	561,05	4,127
480,15	2,456	379,34	1,990	561,74	4,274	561,14	4,097
480,24	2,457	379,67	1,991	561,82	4,533	561,23	4,090
480,34	2,467	379,78	1,991	561,91	4,680	561,31	4,110
480,43	2,447	416,12	2,158	562,00	5,108	561,40	4,176
480,53	2,451	416,22	2,150	**562,03**[a]	**5,780**[a]	561,49	4,213
480,62	2,439	416,32	2,149	**562,03**[a]	**4,120**[a]	561,58	4,280
494,21	2,548	416,43	2,159	562,09	3,950	561,67	4,305
494,31	2,566	416,53	2,151	562,18	3,670	561,76	4,432
494,40	2,556	416,63	2,152	562,27	3,420	561,85	4,640
494,50	2,567	416,74	2,156	562,36	3,350	561,94	4,850
494,59	2,545	416,84	2,158	562,44	3,150	561,97	5,120
494,69	2,521	416,94	2,159	562,53	3,114	562,02	5,635
494,78	2,557	442,42	2,277	562,62	3,058	**562,02**[a]	**6,020**[a]
494,87	2,550	442,52	2,248	—	—	**562,02**[a]	**4,160**[a]
494,97	2,545	442,62	2,278	—	—	562,11	3,840
495,06	2,564	442,72	2,255	—	—	562,20	3,560
560,87	3,715	442,82	2,279	—	—	562,29	3,360
560,96	3,681	442,92	2,280	—	—	562,38	3,250
561,05	3,715	443,02	2,280	—	—	563,08	2,650
561,14	3,722	443,12	2,260	—	—	563,17	2,635
561,23	3,755	443,22	2,281	—	—	563,26	2,603

Continuation table 2

ρ = 336,24 kg/m^3		ρ = 310,36 kg/m^3		ρ = 306,70 kg/m^3		ρ = 300,69 kg/m^3	
T, K	C_V, kJ/kgK	*T*, K	C_V, kJ/kgK	*T*, K	C_V, kJ/kgK	*T*, K	C_V, kJ/kgK
561,31	3,764	483,11	2,500	—	—	563,35	2,570
561,40	3,766	483,21	2,438	—	—	563,44	2,542
561,49	3,821	483,30	2,501	—	—	563,53	2,501
561,58	3,854	483,40	2,501	—	—	563,62	2,502
561,67	3,894	483,49	2,502	—	—	563,70	2,504
561,76	4,016	483,59	2,462	—	—	563,79	2,485
561,85[a]	**4,234[a]**	483,68	2,440	—	—	563,88	2,463
561,85[a]	**3,270[a]**	483,78	2,441	—	—	563,97	2,454
562,02	3,060	483,87	2,504	—	—	564,06	2,463
562,11	2,983	498,45	2,605	—	—	—	—
562,20	2,878	498,55	2,609	—	—	—	—
562,29	2,856	498,64	2,594	—	—	—	—
563,00	2,520	498,73	2,537	—	—	—	—
563,09	2,497	498,83	2,597	—	—	—	—
563,18	2,461	498,92	2,588	—	—	—	—
563,26	2,476	499,02	2,608	—	—	—	—
563,35	2,422	499,11	2,578	—	—	—	—
563,44	2,426	499,20	2,560	—	—	—	—
563,53	2,415	527,46	2,854	—	—	—	—
563,62	2,398	527,55	2,849	—	—	—	—
563,71	2,406	527,64	2,855	—	—	—	—
563,79	2,401	527,73	2,844	—	—	—	—
—	—	527,82	2,851	—	—	—	—
—	—	527,91	2,831	—	—	—	—
—	—	528,01	2,823	—	—	—	—
—	—	528,10	2,807	—	—	—	—
—	—	528,19	2,808	—	—	—	—
—	—	549,90	3,185	—	—	—	—
—	—	549,99	3,152	—	—	—	—
—	—	550,08	3,152	—	—	—	—
—	—	550,17	3,152	—	—	—	—
—	—	550,26	3,219	—	—	—	—
—	—	550,53	3,220	—	—	—	—
—	—	550,62	3,177	—	—	—	—

End table 2

ρ = 336,24 kg/m^3		ρ = 310,36 kg/m^3		ρ = 306,70 kg/m^3		ρ = 300,69 kg/m^3	
T, K	C_V, kJ/kgK	T, K	C_V, kJ/kgK	T, K	C_V, kJ/kgK	T, K	C_V, kJ/kgK
—	—	561,49	4,046	—	—	—	—
—	—	561,58	4,152	—	—	—	—
—	—	561,67	4,164	—	—	—	—
—	—	561,76	4,263	—	—	—	—
—	—	561,85	4,446	—	—	—	—
—	—	561,94	4,646	—	—	—	—
—	—	561,97	4,795	—	—	—	—
—	—	562,01	5,031	—	—	—	—
—	—	562,02	5,260	—	—	—	—
—	—	**562,025**[a]	**5,400**[a]	—	—	—	—
—	—	**562,025**[a]	**3,900**[a]	—	—	—	—
—	—	562,11	3,621	—	—	—	—
—	—	562,20	3,430	—	—	—	—
—	—	562,29	3,223	—	—	—	—
—	—	562,38	3,130	—	—	—	—
—	—	562,47	3,020	—	—	—	—
—	—	562,56	2,920	—	—	—	—
—	—	562,65	2,880	—	—	—	—
—	—	562,73	2,820	—	—	—	—
—	—	600,00	2,257	—	—	—	—
—	—	600,09	2,240	—	—	—	—
—	—	600,18	2,243	—	—	—	—
—	—	600,26	2,250	—	—	—	—
—	—	600,35	2,244	—	—	—	—
—	—	600,43	2,240	—	—	—	—
—		600,52	2,245	—	—	—	—

[a] Bold values are one- C_{V_1} and two-phase C_{V_2} at phase-transition temperature;
[b] Standard uncertainties u are: $u(T) = 7{,}5$ mK; $u(\rho) = 0{,}05$ %; $u(C_V) = 1{,}5$% (level of confidence=0,95).

of state (REFPROP [52]). The temperature dependence of the measured C_V the experimental critical isochore of 306,7 kg $\cdot$ m^{-3} is shown in Fig. 1 together with the values calculated from a scaling-type equation (see below Eq. 9). As one can see from Figs. 1 and 2, for each measured liquid and vapor isochores (ρ), the two-phase C_{V_2} drops discontinuously (abruptly decreases) at the phase transition temperatures (T_S), to a value

corresponding to that of the liquid or vapor in the single-phase region, C_{V_1}. The temperature dependence of the measured two-phase (C'_{V_2}, C''_{V_2}) and single-phase (C'_{V_1}, C''_{V_1}) liquid ($'$) and vapor ($''$) heat capacities along the saturation curve are shown in Figs. 3 and 4 together with the isochoric heat capacity jumps for the liquid ($\Delta C'_V = C'_{V_2} - C'_{V_1}$) and vapor ($\Delta C''_V = C''_{V_2} - C''_{V_1}$) isochores. These figures also include the values calculated from the reference equation of state (REFPROP [52]). The magnitude of the isochoric heat capacity jumps, $\Delta C'_V$ and $\Delta C''_V$, considerably depends on density (therefore, on the phase transition temperature). For near-critical isochores, the values of the isochoric heat capacity jumps, ΔC_V, are very large. As one can see from Figs. 3 and 4 (right), near the critical point $\Delta C'_V \to +\infty$ diverges as $C_{V_2} \propto (T - T_C)^{-\alpha}$ (a scaling law prediction [37, 38]). The measured two-phase C_{V_2} as a function of specific volume V for various near-critical isotherms are shown in Fig. 5. As one can note, the measured two-phase ($C_{V_2} - V$) isotherms are linear functions of specific volume, V, as it is predicted by theory [53] (see also Fig. 6 for selected near-critical isotherms). As will be shown below, the two-phase C_{V_2} provides very useful theoretically important information on the system near the phase- transition and the critical point. One may note (see Fig. 6) that each isotherm started at the saturated liquid specific volume, $V'_S = 1/\rho'_S$, with the value of single-phase saturated liquid heat capacity of C'_{V_1}, then abruptly increases to the two-phase saturated liquid heat capacity C'_{V_2}. A further volume increase leads to a linear

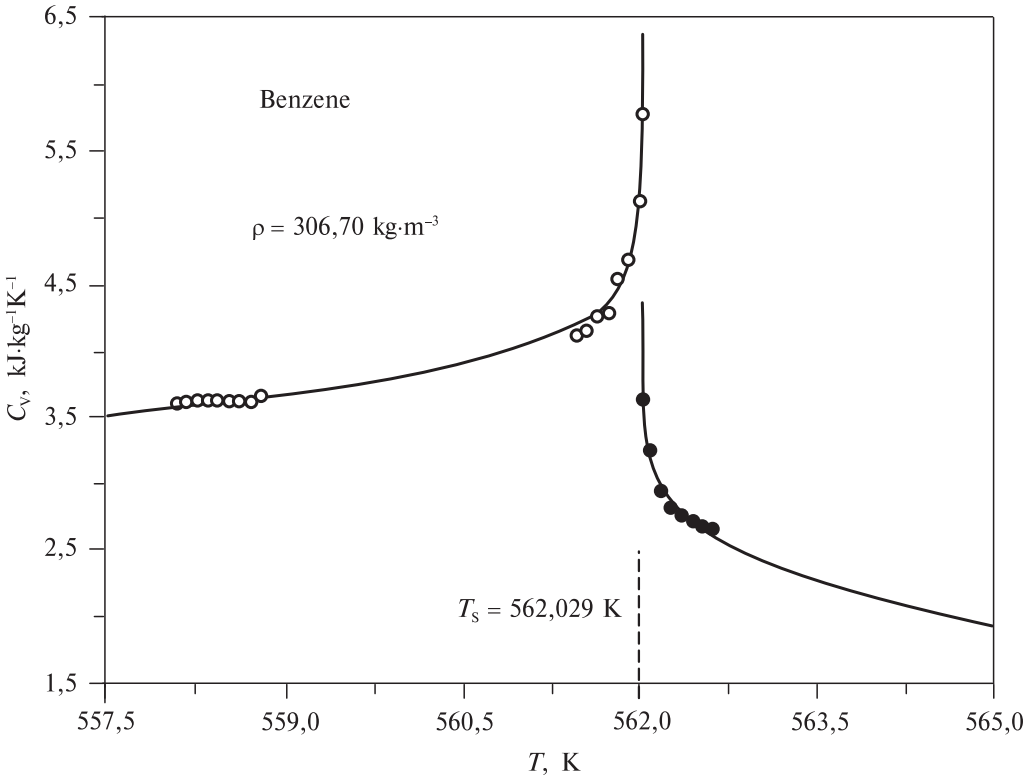

Fig. 1. Measured single- and two-phase isochoric heat capacities of benzene as a function of temperature along the critical isochore of 306,7 kg·m^{-3}:

○ — two-phase heat-capacity; ● — single-phase heat-capacity. The solid lines are calculated from the scaling-type Eq. (9)

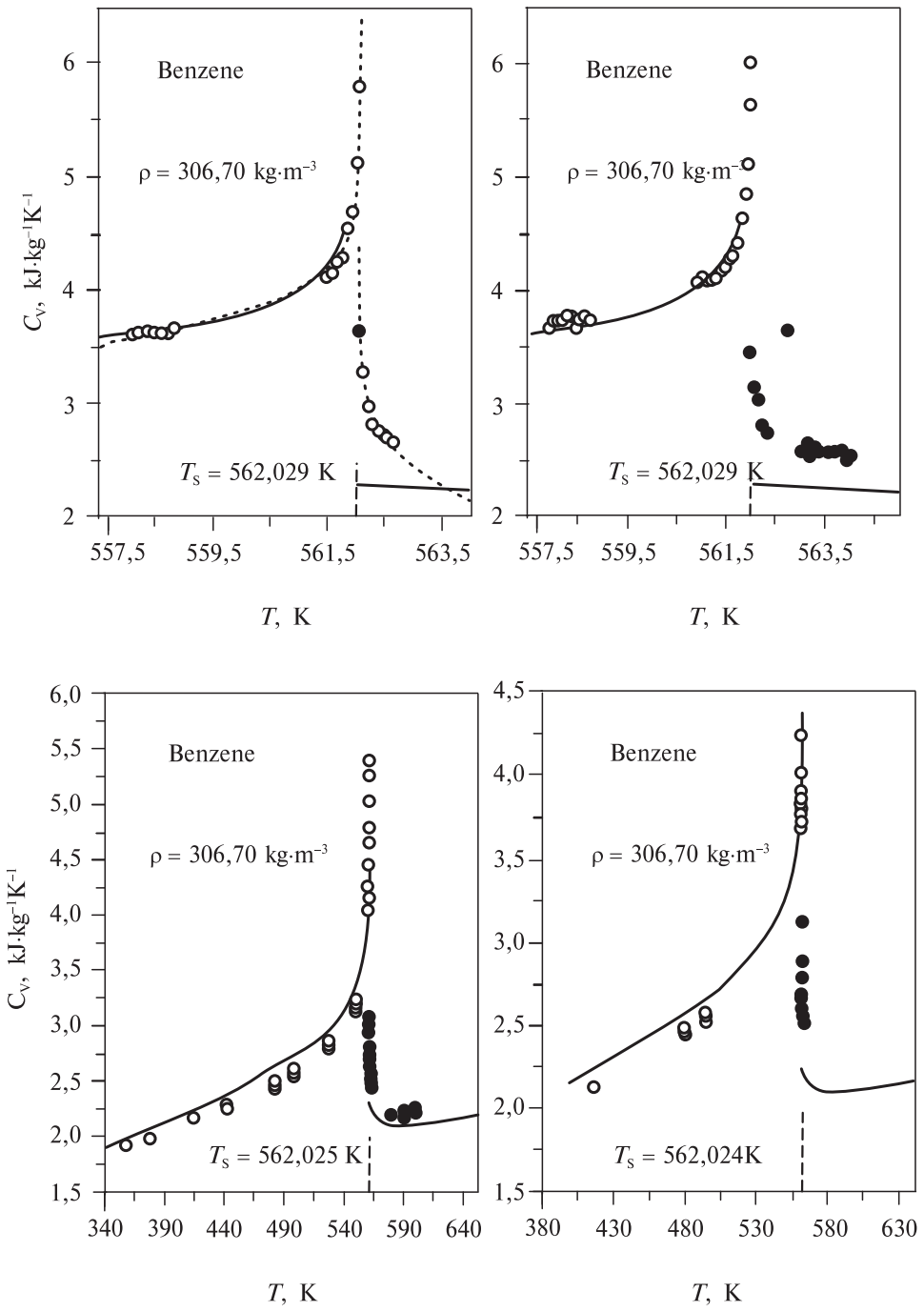

Fig. 2. Measured single- and two-phase isochoric heat capacities of benzene as a function of temperature along the four selected near-critical isochores in the immediate vicinity of the phase transition temperatures together with the values calculated from the reference equation of state REFROP [52]:

○ — two-phase heat-capacity; ● — single-phase heat-capacity. Solid lines are calculated from the reference equation of state [52]. Dashed lines are calculated from the scaling-type equation, Eq. (9)

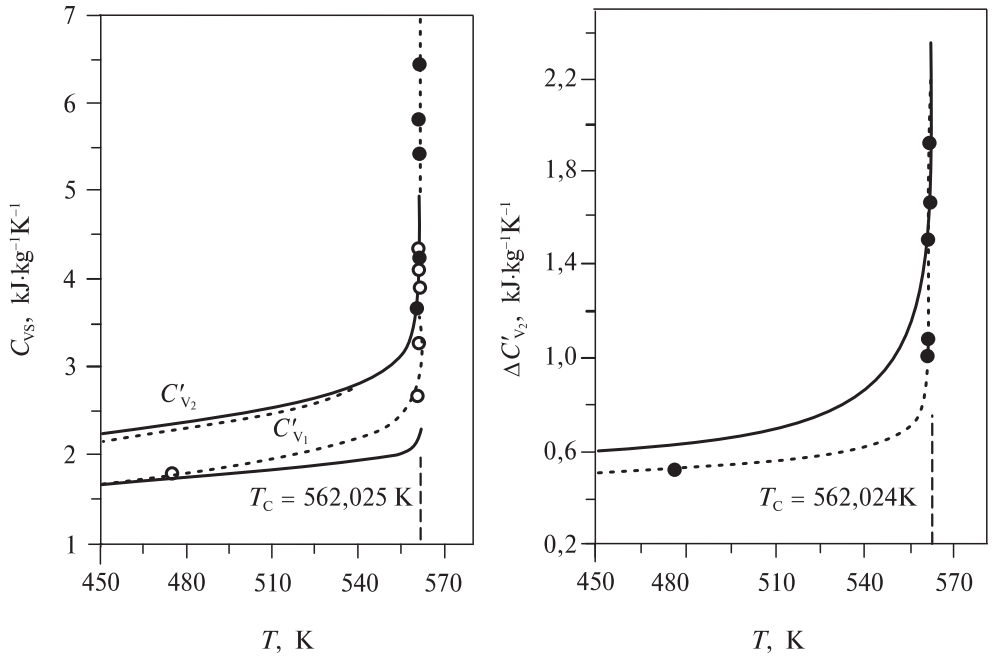

Fig. 3. Measured single- (C'_{V_1}) and two-phase (C'_{V_2}) liquid isochoric heat capacities of benzene as a function of temperature along the L+G coexistence curve near the critical point (*left*) and liquid isochoric heat capacity jumps ($\Delta C'_{V_1}$, *right*) together with the values calculaved from the reference equation of state REFPROP [52]. Dashed lines are calculated from the scaling-type equation

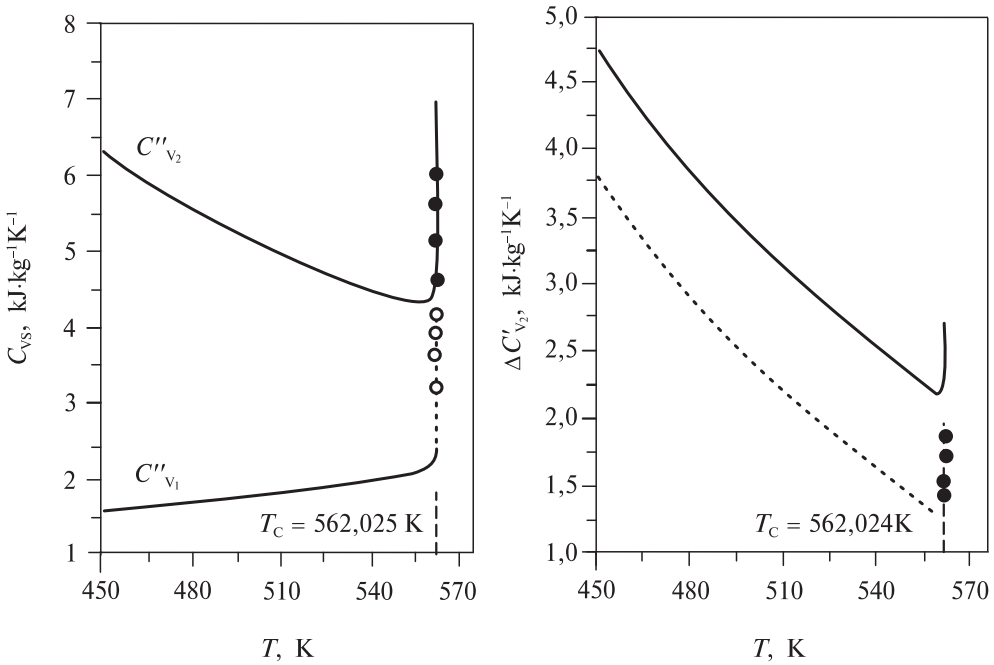

Fig. 4. Measured single- (C''_{V_1}) and two-phase vapor (C''_{V_2}) isochoric heat capacities of benzene as a function of temperature along the L+G coexistence curve near the critical point (*left*) and vapor isochoric heat capacity jumps ($\Delta C''_{V_1}$, *right*) together with the values calculated from the reference equation of state REFPROP [52]

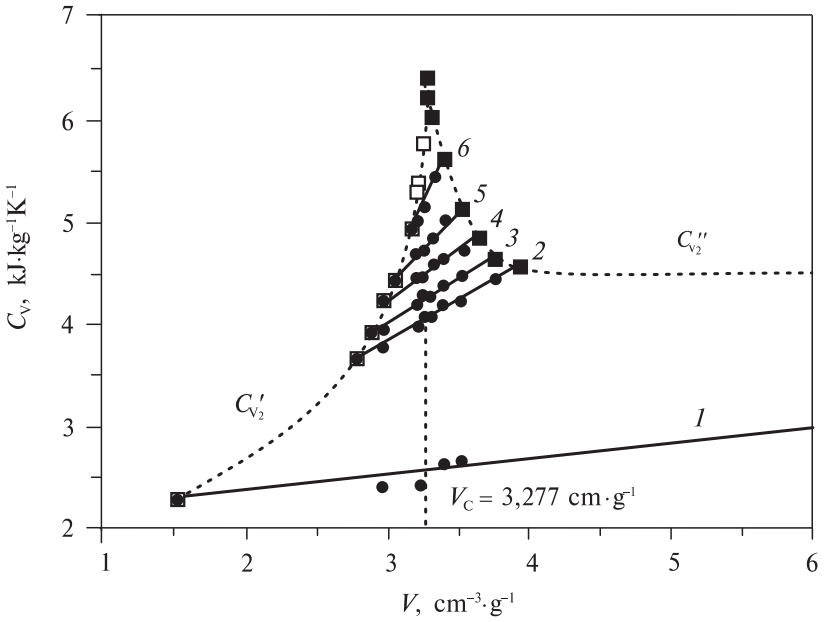

Fig. 5. Measured two-phase isochoric heat capacities of benzene as a function of specific volume V for various selected near-critical isotherms:

□ — two-phase liquid C'_{V_2} at saturation; ■ — two-phase vapor C''_{V_2} at saturation; ●—two-phase C_{V_2} along the fixed isotherms; *1* — 475,91 K; *2* — 561,35 K; *3* — 561,70 K; *4* — 561,85 K; *5* — 561,95 K; *6* — 562,013 K

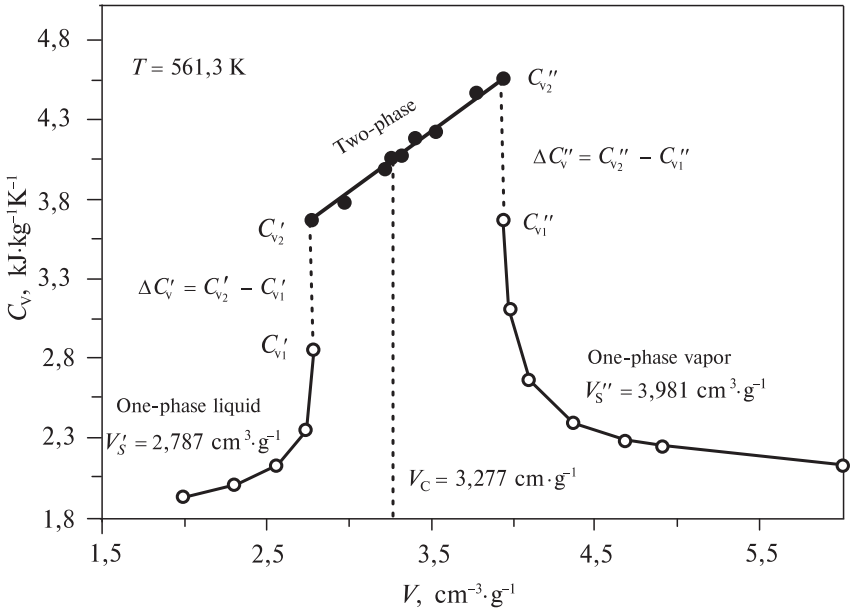

Fig. 6. Experimental single- and two-phase isochoric heat capacities of benzene as a function of specific volume for the near-critical isotherm of 561,3 K:

●—two-phase C_{V_2}; ○— single-phase liquid and vapor heat-capacity; C''_{V_2}—two-phase liquid; C'_{V_2}—two-phase vapor heat-capacities at saturation; C'_{V_1}—single-phase liquid; C''_{V_1}—single-phase vapor heat-capacity at satwration; $\Delta C'_V = C'_{V_2} - C'_{V_1}$— saturated liquid; $\Delta C''_V = C''_{V_2} - C''_{V_1}$saturated vapor isochoric heat capacity jumps

increase of the two-phase heat-capacity until the saturated vapor specific volume, $V''_S = 1/\rho''_S$, is reached at the two-phase saturated vapor heat capacity of C''_{V_2}. Then it abruptly drops to the value of the single-phase saturated vapor heat capacity C''_{V_1}. As we can note, the specific volume dependence of the isochoric heat capacity exhibitsa distinct behavior in various ranges of volume. We experimentally found that between the specific volumes V'_S and V''_S (two-phase region), the two-phase isochoric heat capacity C_{V_2} shows linear behavior. The isothermal two-phase $C_{V_2} - V$ dependence provides very useful scientific information on the temperature behavior of the second temperature derivatives of the vapor-pressure and chemical potential (see below). As Fig. 5 illustrates, the two-phase saturated vapor heat capacity C''_{V_2} shows a «turning point» (a weak minimum) at a specific volume around $V = 4\ \text{cm}^3 \cdot \text{g}^{-1}$. For most simple molecular fluids, such as noble gases, no «turning point» was observed. For other fluids, depending on their molecular structure, the «turning point» is located far from the critical volume V_C and is very weakly pronounced. The location of the «turning point» play san important role in the Yang—Yang parameter determination (see, for example, Ref. 30), i.e., it defines the temperature behavior and the contribution of the second temperature derivatives of the vapor-pressure and chemical potential to the measured total two-phase heat capacity C_{V_2} near the critical point.

Fig. 6 shows the general specific volume dependence of the single- and two-phase C_V values in the liquid and vapor phases for a selected near-critical isotherm of 561,3 K. As one can see from Fig. 6, each isotherm (fixed temperature, T) exhibits two C_V-abrupt points ($\Delta C'_{V_1}$ and $\Delta C''_V$) at saturated liquid (V'_S) and vapor (V''_S) specific volumes. The shape of the $C_V - V$ curve considerably depends on how close is the isotherm to the critical temperature (see Fig. 5). When the temperature (isotherm) approaches the critical value, the difference between V'_S and V''_S decreases, finally for the critical isotherm ($T = T_C$) the specific volumes of the saturated liquid and vapor phases become identical, $V'_S = V''_S = V_C$ (see Fig. 5).

Fig. 7 shows the density dependence of the measured single-phase C_V along two selected supercritical isotherms together with the values calculated from the reference fundamental equation of state (REFPROP [52]). Single-phase isochoric heat capacities are also providing valuable theoretical information on the temperature derivatives $\left(\partial^2 P/\partial T^2\right)_\rho$ of fluids in the supercritical region and at densities of $\approx 2\rho_C$. For example, it is well-known [54—64] that the single-phase $C_V - \rho$ dependence provides very useful information on the qualitative behavior of the P—T-isochores curvature, $\left(\partial^2 P/\partial T^2\right)_\rho$, i.e., the qualitative behavior of the thermodynamic PVT-surface near the critical point. The second temperature derivatives of pressure, $\left(\partial^2 P/\partial T^2\right)_\rho$ and vapor-pressure, $\left(\partial^2 P_S/\partial T^2\right)$, for benzene can be directly calculated from the presently measured values of C_V in the single-phase region as the first density derivative, $\left(\partial C_V/\partial\rho\right)_T$ and the two-phase liquid (C'_{V_2}) and vapor (C''_{V_2}) measurements at saturation as

$$\left(\frac{\partial^2 P}{\partial T^2}\right)_\rho = -\frac{\rho^2}{T}\left(\frac{\partial C_V}{\partial \rho}\right)_T, \tag{4}$$

$$\frac{d^2 P_S}{dT^2} = \frac{C''_{V_2} - C'_{V_2}}{T\left(V'' - V'\right)}. \tag{5}$$

Thus, single- and two-phase C_V measurements as a function of specific volume (or density) are defining the real curvature, $\left(\partial^2 P/\partial T^2\right)_\rho$ and $\left(d^2 P_S/dT^2\right)$, of the $(P\rho T)$ surface and the vapor-pressure $P_S - T$ curve of fluids in the near- and supercritical regions.

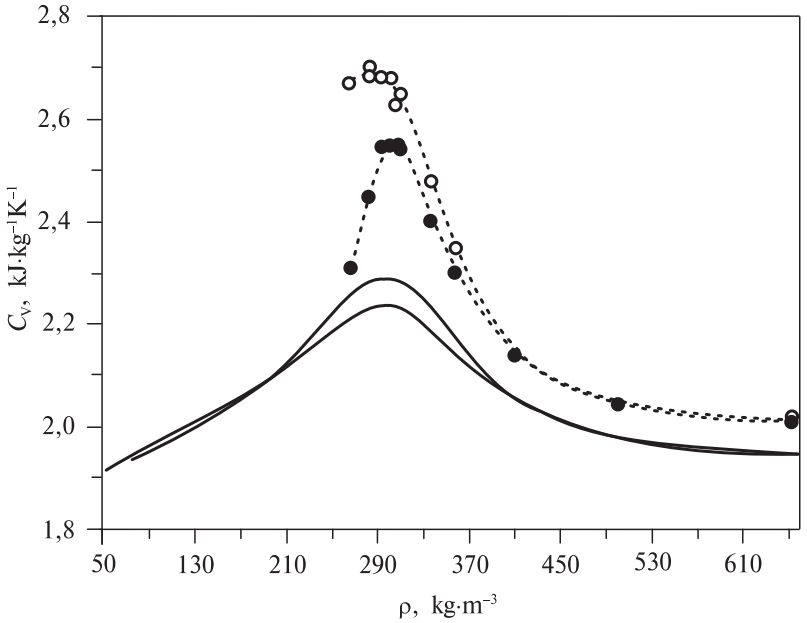

Fig. 7. Measured isochoric heat capacities of benzene as a function of density along the two selected supercritical isotherms together with the values calculated from the reference equation of state REFPROP [52] (solid lines):
○ — T = 562,03 K; ● — T = 564,06 K

As Fig. 7 demonstrates, the sign of the $\left(\partial^2 P/\partial T^2\right)_\rho$ derivative changes from positive (below ρ_C) to negative (above ρ_C) around the critical density, depending on the supercritical isotherms. This means that the $C_V - \rho$ isotherms show a maximum around the critical density along the supercritical isotherms (see Fig. 7). As one can see from Eq. (4), the loci of the C_V extrema, $\left(\partial C_V/\partial\rho\right)_T = 0$, coincide with the loci of the P—T-isochore inflection points, where $\left(\partial^2 P/\partial T^2\right)_\rho = \left(\partial C_V/\partial\rho\right)_T = 0$, [54—60]. The location of the C_V maxima or the P—T-inflection points is changing with increasing temperature (see also our previous publication [54]). Therefore, PVT-data together with C_VVT-measurements are providing very useful theoretical information to develop a functional form of the fundamental equation of state which correctly takes into account the non-classical scaling behaviorof the isochoric heat capacity, $C_V \propto (T - T_C)^{-\alpha}$, and allows to test the predictive capabilities of various theoretical models. Thus, the asymptotic scaling behavior of the temperature dependence of pressure along the critical isochore near the critical point should be as $\Delta P(\rho_C, t) \propto t^{2-\alpha}$, (where $\alpha = 0{,}11$ is the universal critical exponent of the isochoric heat capacity). This means that the pressure and its first temperature derivative, $\gamma_V = \left(\partial P/\partial T\right)_V$, remain finite at the critical point, while the second temperature derivative, $\left(\partial^2 P/\partial T^2\right)_{\rho_C}$, diverges weakly as C_V, i.e., $\left(\partial^2 P/\partial T^2\right)_{\rho_C} \propto t^{-\alpha}$. Both $\left(\partial^2 P_S/\partial T^2\right)$ and $\left(\partial^2 P/\partial T^2\right)_{\rho_C}$ derived from C_V measurements go to infinity at the critical point as $\propto t^{-\alpha}$ (scaling behavior). Therefore, the curvature parts of the equation of state, $\Delta P(\rho, T)$, and the vapor-pressure equation, $\Delta P_S(T)$, should be non-analytical functions of temperature at the critical point.

The present two-phase isochoric heat capacities were used to calculate the values of the saturation heat capacity C_{sat} to compare with the data reported by Chirico and Steele [19]. The measured two-phase heat capacitates C_{V_2} were converted to C_{sat} by means of the well-known thermodynamic relation

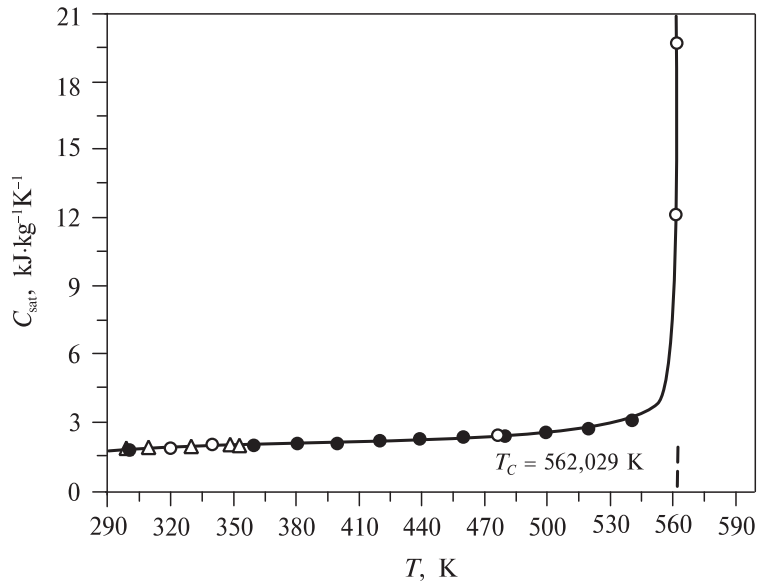

Fig. 8. Saturation heat capacity (C_{sat}) of benzene as a function of temperature derived from the present experimental two-phase heat capacities (C_{V_2}) and directly measured saturated liquid specific volumes and vapor–pressure temperature derivatives (Eq. 6):
○ — this work; ● — Chirico and Steele [19]; Δ — Oliver et al. [65]. Solid line is calculated from the fundamental equation of state (REFPROP [52])

$$C_{sat} = C_{V_2} + T\left(\frac{dV}{dT}\right)\left(\frac{dP_S}{dT}\right), \tag{6}$$

where the temperature derivative $\left(\frac{dP_S}{dT}\right)$ was directly measured in the present work (these data together with the *PVT*-measurements will be published separately), while the values of $\left(\frac{dV}{dT}\right)$ were calculated from the present saturated specific volume data. The derived values of the saturation heat— capacity C_{sat} (Eq. 6) together with the data reported by Chirico and Steele [19] and Oliver et al. [65] are shown in Fig. 8. As one can see from Fig. 8, the present results for C_{sat} derived from the directly measured two-phase C_{V_2} are in excellent agreement with the reported data by Chirico and Steele [19] and Oliver et al. [65] (within 2%). This is an additional confirmation of the reliability, accuracy, and thermodynamic consistency of the present measurements (C_{V_2}, V'_S, V''_S) for benzene.

Saturated Liquid (ρ'_S) and Vapor (ρ''_S) Densities and Phase Transition Temperatures (T_S) from Isochoric Heat capacity measurements and Liquid—Gas Coexistence Curve Asymmetry

The phase transition temperatures (T_S) derived from the present C_V-abruption points (see Figs. 1 and 2) for each measured liquid and vapor isochores are shown in Fig. 9 in $T_S - \rho_S$ coordinates together with the reported data. As it was mentioned above, the isochoric heat capacity exhibits a discontinuity upon intersecting the liquid—gas phase transition temperature (see Figs. 1 and 2) for each measured isochore. Also, the

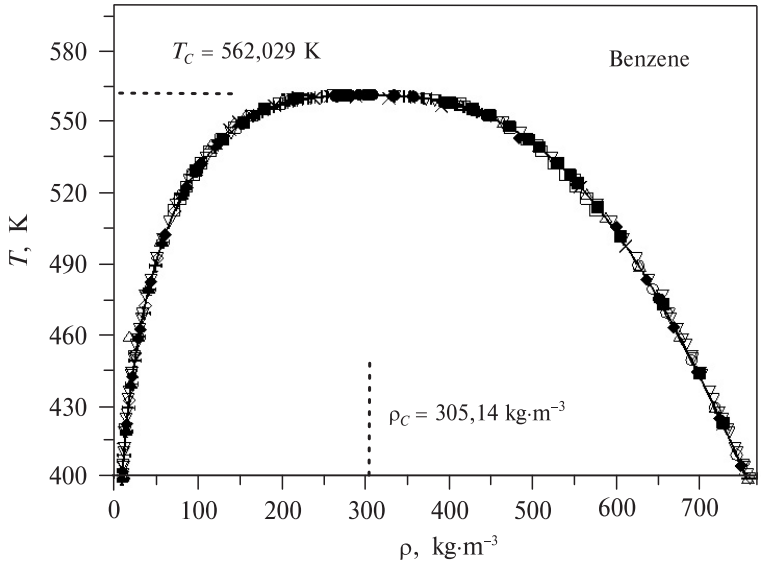

Fig. 9. Measured values of the saturated liquid- and vapor-densities from calorimetric (C_V) experiments together with reported data:

● — this work; ○ − Hales and Townsend [66]; □ − Skaates and Kay [67]; × −Chirico and Steele [19]; Δ — Hales and Gundry [68]; ◊ — Connolly and Kandalic [69]; ♦ — Kooner and Van Hook [70]; ∇ − Campbell and Chatterjee [71]; + − Artukhovskaya et al. [72]; Akhundov and Abdullaev [73]; ✠ — Gorbunova et al. [74];|−Straty et al. [75]. Solid line is calculated from the scaling equation (7)

phase transition temperatures $T_S(\rho)$ for each measured liquid and vapor density (isochore) ρ very clearly exhibit break points of the slopes, $(dT/d\tau)$, on the thermograms. This is an additional confirmation of the accuracy and reliability of the method and of the measured saturated density data for benzene. For liquid isochores, far from the critical isochore, the phase transition temperatures $T_S(\rho)$ were also confirmed using the barogram break points (P—T-isochore break points).

The «complete» scaling theory developed by Fisher and Orkoulas [76] shows that the strength of the Yang—Yang critical anomaly parameter, $R_\mu = \dfrac{C_{V\mu}}{C_{VP} + C_{V\mu}}$, (see below) can also be determined as $R_\mu = a_3/(1+a_3)$, where a_3 is the system —dependent asymmetry coefficient of the liquid—gas coexistence curve diameter of real fluids. The pressure mixing coefficient [76] a_3 is inducing a new more dominant singularity term ($\propto t^{2\beta-1}$) of the liquid + gas coexistence diameter [77]. For real fluids, $R_\mu \neq 0$ and it determines the details of the intermolecular interactions ($a_3 \neq 0$). For «incomplete» scaling models, $a_3 = 0$ and, therefore, $R_\mu = 0$. As it was shown by Orkoulas et al. [80], the Yang—Yang anomaly strength parameter R_μ related to the asymptotic critical amplitude B_0 of the liquid—gas coexistence curve and the «complete» scaling term amplitude B_4 as $R_\mu = B_4/B_0^2$ (see below). Therefore, Yang—Yang anomaly strength parameter R_μ is directly related to the singular diameter criticality as discussed below and can be also estimated from the asymmetry coefficients (B_2 and B_4) of the coexistence curve or the diameter singularity. The present saturated liquid and vapor density data (T_S, ρ_S' and ρ_S'') near the critical point of benzene, determined in the calorimetric C_{V_2} experiments, were used to estimate the Yang—Yang anomaly strength parameter, R_μ.

According to the renormalization group theory [79], («incomplete» scaling) of liquid—gas critical phenomena, the first temperature derivative of the coexistence — curve diameter, $(d\rho_d/dT)$, where $\rho_d = (\rho'_S + \rho''_S)/2\rho_C$, diverges as the isochoric heat capacity $t^{-\alpha}$ (see also Refs. [80—82]). The theory of «complete» scaling [76, 80, 83] predicts a «2β–1» anomaly of the coexistence curve diameter singularity, $(d\rho_d/dT) \propto t^{2\beta-1}$, i.e., liquid—gas coexistence densities can be represented by

$$\Delta\rho = \pm B_0 t^{\beta} \pm B_1 t^{\beta+\Delta} \pm B_2 t^{1-\alpha} - B_3 t + B_4 t^{2\beta}, \quad (7)$$

where $B_i (i = 0,4)$ are the system-dependent critical amplitudes. In Eq. (7), $\pm B_0 t^{\beta}$ is the asymptotic (symmetric) term, $\pm B_1 t^{\beta+\Delta}$ is the non-asymptotic (symmetric Wegner's correction) term, $\pm B_2 t^{1-\alpha}$ is the weak «singular diameter» (the first non-analytical contribution to the liquid—gas asymmetry predicted by «incomplete» scaling), $B_4 t^{2\beta}$ is the non-analytical contribution of the liquid—gas asymmetry (a new «complete» scaling term, more dominant diameter singularity term), and $B_3 t$ is the (classical) rectilinear diameter. Eq. (7) was directly fitted to the presently measured saturated liquid and vapor densities (ρ_S and T_S) without any constrains to the system-dependent critical amplitudes, $B_i (i = 0,4)$. The derived values of the fitting parameters (critical amplitudes) B_i for benzene are: $B_0 = 1{,}4934$, $B_1 = 1{,}6265$, $B_2 = 10{,}6661$, $B_3 = 10{,}1289$, and $B_4 = -1{,}5225$. Therefore, the estimated Yang—Yang anomaly strength parameter is $R_\mu = B_4/B_0^2$. Thus, the «complete» scaling parameter $B_4 < 0$ is negative, which means that the contribution of the chemical potential to the measured two-phase C_{V_2} is negative and $C_{V_\mu} \to -\infty$ at the critical point (see the next section below). This is consistent with the negative divergence of the second temperature derivative of the chemical potential $d^2\mu/dT^2$ derived from the heat capacity measurements (see below).

The value of the system-dependent asymmetry parameter of the liquid-gas coexistence curve derived from $R_\mu = a_3/1 + a^3$ is $a^3 = -0{,}406$. However, the values of the fitting parameters B_1 strongly depend on the fitting temperature range and other fitting procedures. Unfortunately, theory cannot predict the range of temperature where the «complete» scaling theory is valid. Therefore, this method of the Yang—Yang anomaly strength (R_μ) and asymmetry parameter (a^3) determination has a large uncertainty.

As one can see from Eq. (7), the effect of the Yang—Yang anomaly strength, $R_\mu = C_{V\mu}/(C_{VP} + C_{V\mu})$ or $R_\mu = B_4/B_0^2$, on the coexistence curve diameter is given by [76, 77, 80, 83—85]

$$\rho_d = 1 + (B_2 t^{1-\alpha} - B_3 t + B_4 t^{2\beta}), \quad (8)$$

where the «complete» scaling asymmetry parameter can be also defined as $B_4 \propto A_\mu/A_P$ [76, 77], A_μ and A_P are the asymptotic critical amplitudes of the second temperature derivatives of chemical potential $(d^2\mu/dT^2)$, and vapor-pressure (d^2P_S/dT^2), respectively. A Yang—Yang anomaly implies that the leading correction, $\rho_d \propto B_4 t^{2\beta}$, (the «complete» theory correction), would dominate the previously expected $\rho_d \propto B_2 t^{1-\alpha}$ correction [76, 80, 83—85] («incomplete» theory correction), where $2\beta < (1 - \alpha)$. Therefore, the first temperature derivative of the coexistence curve diameter diverges as the isochoric heat capacity $(d\rho_d/dT) \propto t^{1-\alpha}$ and as predicted by the «complete» scaling $(d\rho_d/dT) \propto t^{2\beta-1}$ ($2\beta - 1 \approx -0{,}352$). In other words, the divergence of the liquid—gas coexistence curve diameter is controlled by two terms, the «incomplete» $B_2 t^{1-\alpha}$ and «complete» $B_4 t^{2\beta}$ scaling terms, like the two-phase C_{V_2} divergence consists of the vapor-pressure (C_{VP}) and chemical potential ($C_{V\mu}$) parts (see below). In the present work we used the simultaneously

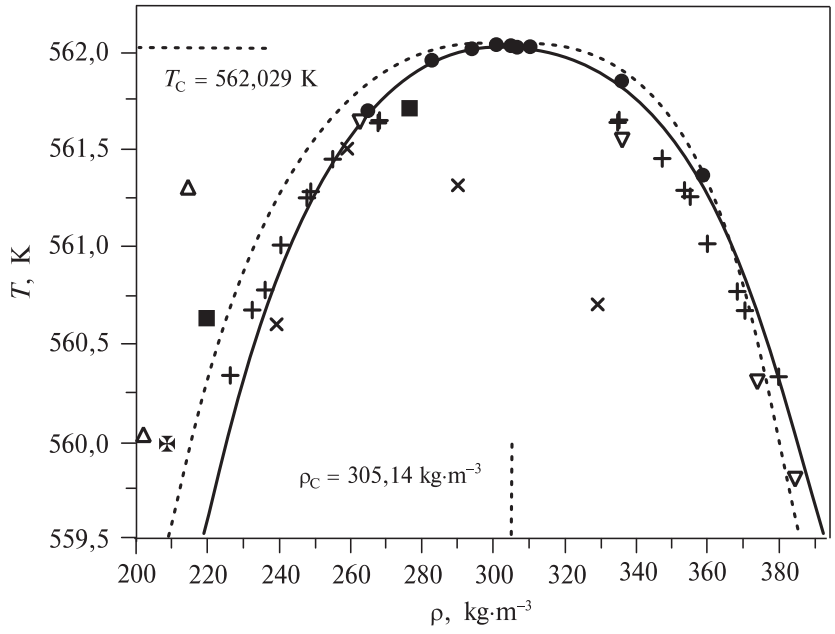

Fig. 10. Detailed view of the experimental L+G coexistence curve shape (top, asymptotic region) near the critical point together with reported data. Symbols are the same as in Fig. 9. Dashed line is calculated from the scaling-type equation (7)

measured two-phase C_{V_2} and saturated liquid and vapor densities (ρ_S', and ρ_S'') for benzene to estimate the value of the Yang—ang anomaly strength parameter, R_μ, through the asymmetric parameters a_3 and B_4 as $R_\mu = a_3/(1 + a_3)$ or $R_\mu = B_4/B_0^2$ with some physically meaningful constrains on the values of B_4, B_3, and B_2 (see below). The liquid—gas coexistence curve asymmetry near the critical point was comprehensively studied by Cerdeiriña et al. [77] and Losada-Perezand Cerdeiriña [85].

It has been shown earlier [86, 87], that the «incomplete» singular diameter (asymmetric parameter) B_2 and the classical rectilinear diameter parameter B_3 in Eqs. (7) and (8) are directly related to the two-phase isochoric heat capacity asymptotic critical amplitude A_0^- and fluctuation-induced «critical background» parameter B_{cr} by the equation

$$\frac{C_V}{k_B} = A_0^- t^{-\alpha}\left(1 + A_1^- t^{\Delta}\right) - \frac{B_{cr}}{k_B}, \tag{9}$$

where k_B is the Boltzmann's constant. The explicit relations (see below, Eq. 11) between the coefficients A_0^-, B_{cr}, B_2, B_3, B_4, and B_0 were studied previously by Wang and Anisimov [87]. The present single- and two-phase C_V data for benzene along the critical isochore (Table 2, Fig. 1) were fitted to Eq. (9). The derived values of the critical amplitude for benzene are: $A_0^+ = 3{,}0910$, $A_1^+ = -28{,}7545$, $B_{cr}^+ = -2{,}5623$ for ($T > T_C$), and $A_0^- = 5{,}8963$, $A_1^- = -7{,}5571$, $B_{cr}^- = -3{,}1754$ for ($T < T_C$). It is very difficult to accurately estimate the value of the fluctuation-induced «critical background» parameter B_{cr}/k_B by using the fitting procedure, because the empirical determination of the fitting parameter strongly depends on the input data, for example, on the fitting temperature range, weight of the experimental data, etc. In general, the regular part of the scaling relation (9) contains

the analytical classical term, the ideal gas contribution, and the fluctuation-induced regular parts, which are very difficult to identify empirically (Perkins et al. [28]).

According to the «complete» scaling theory, the coexistence curve diameter (Eq. 8) can be represented as [87]:

$$\rho_d - 1 = \frac{a_3}{1+a_3} B_0^2 t^{2\beta} - b_2 \left[\frac{A_0^-}{(1-\alpha)} t^{1-\alpha} - \frac{B_{cr}}{k_B} t \right], \tag{10}$$

where a_3 and b_2 are the system dependent asymmetry coefficients. The values of the coexistence curve amplitudes (B_2, B_3, and B_4, Eq. 7) are related to the isochoric heat capacity parameters (A_0^- and B_{cr}, Eq. 9) as [87]

$$B_2 = -b_2 \frac{A_0^-}{(1-\alpha)}; \; B_3 = -b_2 \frac{B_{cr}}{k_B}; \; B_4 = \frac{a_3}{1+a_3} B_0^2. \tag{11}$$

As one can see from Eq. (11), the critical amplitude of the two-phase isochoric heat capacity along the critical isochore (A_0^-), fluctuation-induced «critical background» term (B_{cr}), and the coexistence curve amplitudes (B_0, B_2, B_3, and B_4) are dependent on each other. As it follows from Eq. (11), Yang—Yang anomaly strength parameter R_μ is defined through the asymmetric parameter a_3 as $R_\mu = a_3/(1 + a_3)$ or through a non-analytical contribution of the liquid—gas asymmetry (a new «complete» scaling term B_4) and the asymptotic (symmetric) term B_0, $R_\mu = B_4/B_0^2$. Thus, the pressure mixing coefficient a_3 in the «complete» scaling theory can be directly determined experimentally by simultaneously measuring both sides of the coexistence curve (saturated liquid and vapor densities) near the critical point and the two-phase isochoric heat capacity data (asymptotic critical amplitude of heat capacity, A_0^- and the back ground term B_{cr}). Equation (7) together with constrains (11) was applied to the present saturated liquid and vapor densities (T_S, ρ_S', ρ_S'') derived from the two-phase C_V experiments for benzene in the critical region. The derived values for benzene are $B_0 = 1{,}6714$; $B_1 = 0{,}0306$; $a_3 = -0{,}4152$; $b_3 = -0{,}6393$. As one can see, the asymmetric parameter $a_3 = -0{,}4152$ is close to the value of $a_3 = -0{,}406$ derived from direct fitting procedure without constrains (see above). In general, the singular liquid—gas coexistence curve diameter (Eq. 10) contains only two adjustable parameters a_3 and b_2. As we can note, the asymmetry coefficients for benzene have the same negative sign, $a_3 < 0$ and $b_2 < 0$. This means that the «complete», $\frac{a_3}{1+a_3} B_0^2 t^{2\beta} < 0$ and «incomplete», $b_2 \frac{A_0^-}{(1-\alpha)} t^{1-\alpha} > 0$, scaling terms in Eq. (7) have opposite signs (i.e., opposite contribution). Therefore, for benzene the singularity of the coexistence curve diameter ρ_d is shared between the «incomplete» $t^{1-\alpha}$ and «incomplete» $t^{2\beta}$ terms. Their respective contributions are shown in Fig. 11. As one can see, the singular diameter behavior is basically controlled by the «complete» scaling term $t^{2\beta}$. For benzene, the coexistence curve diameter exhibits a considerable deviation from the rectilinear diameter in the immediate vicinity of the critical point, because the contribution of the «complete» scaling term is dominating. For some fluids, both asymmetric parameters a_3 and b_2 of the coexistence curve diameter are positive (see, for example, *n*-pentane, *n*-heptane, SF_6, and R-113) [87]. For these fluids, the contribution of the «complete» and «incomplete» terms is opposite (see Eq. 10), namely, $t^{2\beta}$ is positive, and $t^{1-\alpha}$ is negative. An opposite behavior, i.e., a negative contribution of $t^{2\beta}$ and a positive

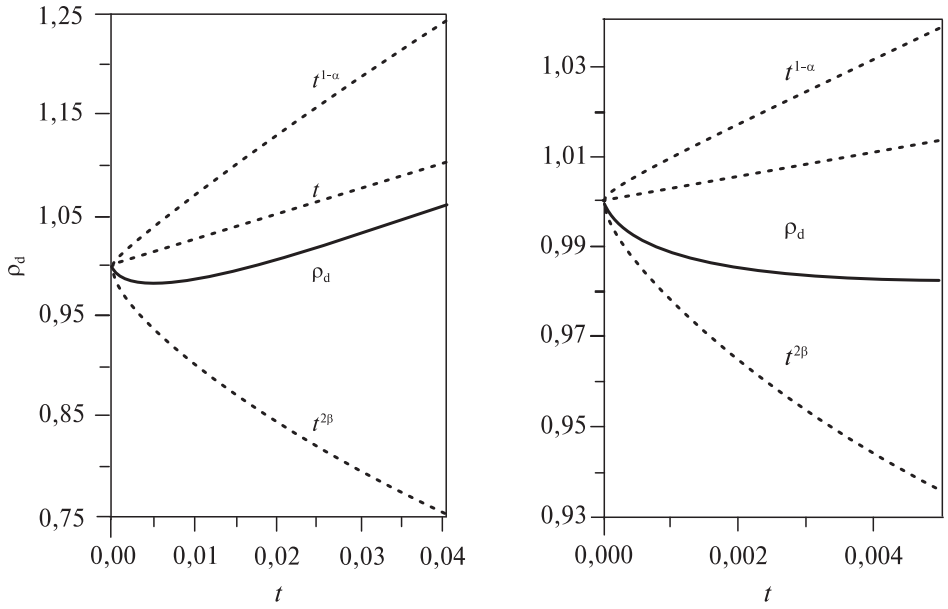

Fig. 11. The non-analytical (scaling) «incomplete» $B_2 t^{1-\alpha}$ (*a*) and «complete» $B_4 t^{2\beta}$ (*b*) contributions to the coexistence curve singular diameter of benzene from the present isochoric heat capacity measurements near the critical point. Solid and dashed lines are calculated from the scaling equation (10)

contribution of $t^{1-\alpha}$ terms, was found for neon, methane, nitrogen, ethane, and hard-core square-well fluids [87].

Two-Phase Isochoric Heat Capacities and Second Nemperature Derivatives (d^2P_S/dT^2) and $(d^2\mu_S/dT^2)$ Near the Critical Point

Forthe two-phase (liquid—gas coexistence) isochoric heat capacity, the Yang and Yang [53] relation is

$$C_{V_2} = -T\frac{d^2\mu}{dT^2} + VT\frac{d^2P_S}{dT^2}, \tag{12}$$

where C_{V_2} is the two-phase isochoric heat capacity and V is the specific volume. According to Eq. (12), the two-phase isochoric heat capacity C_{V_2} is a linear function of specific volume V along each fixed isotherm T, the slope of which is equal to $T\left(d^2P_S/dT^2\right)$, while the intercept for $V=0$ is related to $-T\left(d^2\mu/dT^2\right)$. Rapid increase of the slope of C_{V_2}—V isotherms (see also Fig. 5), as the critical temperature approaches, is the result of the increasing second temperature derivative, $\left(d^2P_S/dT^2\right)$. As one can see from Eq. (12), the saturated two-phase liquid (C'_{V_2} and V') and vapor (C''_{V_2} and V'') heat capacities and specific volumes are related to the second temperature derivatives $\left(d^2P_S/dT^2\right)$ and $\left(d^2\mu/dT^2\right)$ as

$$\frac{d^2P_S}{dT^2} = \frac{C''_{V_2} - C'_{V_2}}{T\left(V'' - V'\right)} \text{ and } \frac{d^2\mu}{dT^2} = \frac{V''C'_{V_2} - V'C''_{V_2}}{T\left(V' - V''\right)}, \tag{13}$$

where V'' and V' are, respectively, the vapor and liquid specific volumes at saturation, corresponding to a given temperature T. The measured properties (T_S, V, C'_{V_2}, V'', C''_{V_2}) on the right-hand sides of Eqs. (13) were used to calculate the temperature derivatives

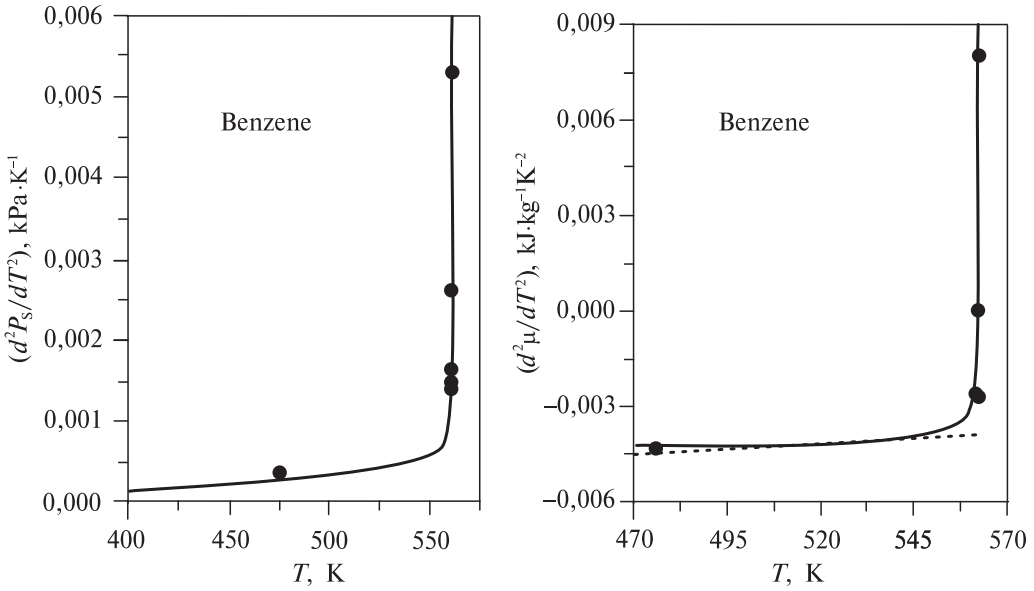

Fig. 12. Measured and calculated values of the second temperature derivative of vapor-pressure (*left*) and chemical potential (*right*) for benzene:

● – $\left(d^2P_S/dT^2\right)$ from the present two-phase C_{V_2} measurements (Eqs. 12 and 13); Solid line is calculated from the reference equation of state [52]. Dashed line is calculated from the correlation of Chirico and Steele [19]

$\left(d^2P_S/dT^2\right)$ and $\left(d^2\mu/dT^2\right)$ for benzene. We also used the Yang—Yang equation Eq. (12) for different isotherms to directly fit the measured C_{V_2} values for the calculation of the second temperature derivatives $\left(d^2P_S/dT^2\right)$ and $\left(d^2\mu/dT^2\right)$. The derived values of $\left(d^2P_S/dT^2\right)$ and $\left(d^2\mu/dT^2\right)$ as functions of temperature are shown in Fig. 12, which also includes the values of $\left(d^2P_S/dT^2\right)$ calculated from the reference equation of state (REFPROP [52]) by twice differentiating the vapor-pressure equation. Fig. 12 demonstrates, that the values of $\left(d^2P_S/dT^2\right)$ derived from the present two-phase C_{V_2} measurements are rapidly increasing upon approaching the critical point, showing a singular behavior. As can also be noted from Fig. 12 (right), the values of $\left(d^2\mu/dT^2\right)$ derived from two-phase C_{V_2} measurements are positively diverging at the critical point like $\left(d^2P_S/dT^2\right)$. Figure 12 (right) also includes the values of $\left(d^2\mu/dT^2\right)$ reported by Chirico and Steele [19] from two-phase heat-capacity measurements, and one can see that far from the critical point the agreement between the present and published data [19] is good, while near the critical point the discrepancy is qualitatively different. The data by Chirico and Steele [19] are very slowly and monotonously increasing without any anomaly at the critical point. The non-analytical vapor-pressure equation (REFPROP [52]) correctly predicts the behavior of $\left(d^2P_S/dT^2\right)$ near the critical point, although the leading asymptotical behavior of $\left(d^2P_S/dT^2\right)$ for this equation is $\left(d^2P_S/dT^2\right) \propto t^{-0,5}$, which is different from the theoretically predicted power law behavior of $\left(d^2P_S/dT^2\right) \propto t^{-0,11}$ [37]. However, the vapor-pressure equation in REFPROP [52] can be successfully used for practical applications. Thus, the second temperature derivative of the vapor pressure, $\left(d^2P_S/dT^2\right)$, can be accurately estimated from the two-phase C_{V_2} measurements and in good agreement with the values derived from twice differentiating the vapor pressure

curve in the wide temperature range, including the critical point. Figure 12 (right) also demonstrates that the second temperature derivative of chemical potential, $\left(d^2\mu/dT^2\right)$, derived from the present two-phase isochoric heat capacity C_{V_2} measurements, in contrast with the «incomplete» scaling theory prediction, positively diverges at the critical point and disagrees with the data reported by Chirico and Steele [19] in the immediate vicinity of the critical point, although far from the critical point the agreement is good enough.

Yang—Yang Anomaly Strength Parameter

It is well-known [37, 76, 80], that the two-phase isochoric heat capacity C_{V_2} (left side of the Eq.12) is diverging at the critical point as a simple power law $C_{V_2} \infty t^{-\alpha}$. Therefore, the right-hand side of Eq. (12) should also diverge as $\infty t^{-\alpha}$. It is apparent that the divergence of C_{V_2} can be caused by the divergence of C_{V_2} or $C_{V\mu}$, or both of them in the Yan—Yang relation

$$C_{V_2} = C_{V\mu} + C_{VP}, \tag{14}$$

where $C_{VP} = V_C T \dfrac{d^2 P_S}{dT^2}$ is the vapor pressure and $C_{V\mu} = -T \dfrac{d^2\mu}{dT^2}$ is the chemical potential parts (contributions) of the total measured two-phase isochoric heat capacity C_{V_2}. As one can see from Fig. 12, the divergence of C_{V_2} for benzene is caused by the positive divergences of both derivatives, $\left(d^2P_S/dT^2\right)$ and $\left(d^2\mu/dT^2\right)$. However, the contributions are opposite in sign at the critical point: $C_{VP} > 0$, while $C_{V\mu} < 0$. The temperature dependences of the vapor pressure C_{VP} and chemical potential $C_{V\mu}$ contributions to the

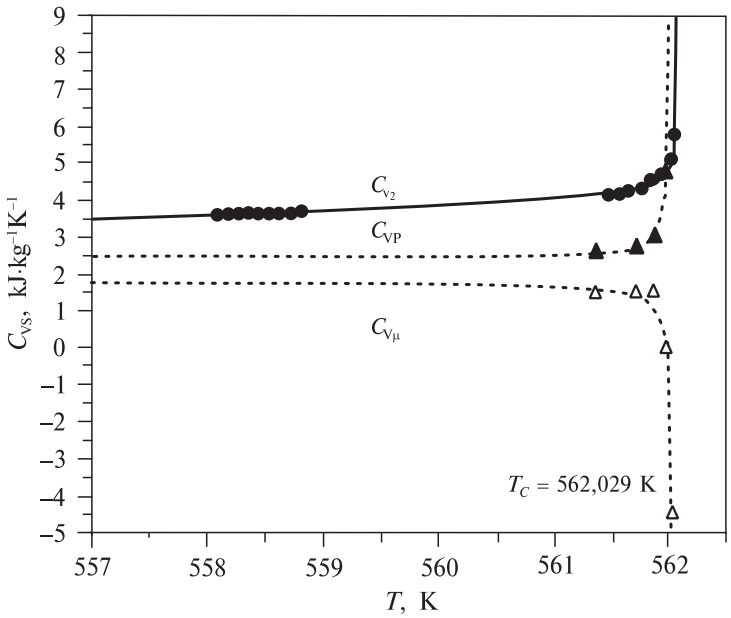

Fig. 13. Chemical potential $C_{V\mu}$ and vapor-pressure C_{VP} contributions of the two-phase isochoric heat capacities C_{V_2} of benzene as a function of temperature:

● — C_{V_2} along the critical isochore of 306,7 kg · m^{-3}; Δ — chemical potential contribution, $C_{V\mu} = -T\left(d^2\mu/dT^2\right)$;

▲ — vapor-pressure contribution, $C_{VP} = TV_C\left(d^2\mu/dT^2\right)$. Solid line is calculated from the scaling-type equation (9)

total measured two-phase heat capacity C_{V_2} are shown in Fig. 13. The contribution of $\left(d^2P_S/dT^2\right)$ and $\left(d^2\mu/dT^2\right)$ to the divergence of C_{V_2} can be quantitatively estimated by the Yang—Yang anomaly strength parameter R_μ (Yang—Yang anomaly in fluid criticality) near the critical point [76, 80]. The strength of the Yang—Yang anomaly R_μ was for the first time defined by Fisher and co-authors [76, 80, 83, 84] as $R_\mu = A_\mu/(A_\mu + A_P)$, where A_μ and A_P are the asymptotic amplitudes of the singularity of $-T\left(d^2\mu/dT^2\right) \approx A_\mu t^{-\alpha}$ and $TV_C\left(d^2P_S/dT^2\right) \approx A_\mu t^{-\alpha}$. By definition [80], the Yang—Yang anomaly strength parameter is $R_\mu \equiv \lim_{t\to 0} \dfrac{C_{V\mu}}{C_{VP} + C_{V\mu}} = \dfrac{A_\mu}{A_P + A_\mu}$. Yang—Yang anomaly strength parameter, R_μ, measures the contribution of the chemical potential $C_{V\mu}$ to the total experimental two-phase heat capacity C_{V_2} singularity relative to that of the vapor-pressure C_{VP} contribution in an asymptotic limit of $(T \to T_C)$. In the earlier works [76, 80], previous scaling descriptions have been extended by introducing the pressure ΔP into the ordering field, $h_1 = a_1\Delta\mu + a_2\Delta T + a_3\Delta P$. Theoretically, the parameter R_μ is related solely to the pressure mixing coefficient a_3, or to the coexistence curve diameter asymmetry coefficient B_4 [76] (see Eqs. 7 and 8 above), as $R_\mu = a_3/(1 + a_3)$ or $\left(d^2\mu/dT^2\right) = -a_3/(1 + a_3)$, $(C_V/T) = -a_3\left(d^2P_S/dT^2\right)$. The Yang—Yang anomaly strength parameter R_μ is anon-universal (individual) parameter of fluids. Therefore, its magnitude and sign strongly depend on the molecular size, shape, symmetry, departures from near-spherical form [76, 80, 84]. If $R_\mu = 0$, then, $A_\mu = 0$, the divergence of the two-phase isochoric heat capacity C_{V_2} caused only by the divergence of $V_C T\left(d^2P_S/dT^2\right)$, while $-T\left(d^2\mu/dT^2\right)$ remains finite as the «incomplete» scaling theory predicts [88—90] (see also Chirico and Steele [19]). If $R_\mu \neq 0$, i.e., $A_\mu \neq 0$, the divergence of the two-phase isochoric heat capacity C_{V_2} in Eq. (12) is caused by the divergence of both derivatives or by just one: $-T\left(d^2\mu/dT^2\right)$. The detailed study of the Yang—Yang parameter for various molecular liquids is presented in our recent review [30]. We have developed a new method for the Yang—Yang anomaly strength parameter R_μ determination [30, 91] using the directly measured two-phase saturated liquid (C'_{V_2}) and vapor (C''_{V_2}) heat capacities and saturated liquid (V') and vapor (V'') specific volumes at a given temperature (T) by avoiding the fitting procedure as

$$R_\mu = \frac{C_{V\mu}}{C_{VP} + C_{V\mu}} = \frac{V''C'_{V_2} - V'C''_{V_2}}{C''_{V_2}\left(V'' - V_C\right) - C''_{V_2}\left(V' - V_C\right)}, \tag{15}$$

where we used relations (13) to calculate the values of C_{VP} and $C_{V\mu}$. As one can see from Eq. (15), the sign of the Yang—Yang parameter R_μ is defined by the sign of the numerator $(V''C'_{V_2} - V'C''_{V_2})$ because the denominator is always positive $(C''_{V_2} > 0, V'' > V_C$, and $V' < V_C)$. When the critical temperature approaches $(T \to T_C)$, then $V'' \to V' \to V_C$, therefore, $(V''C'_{V_2} - V'C''_{V_2}) \to V_C(C'_{V_2} - C''_{V_2}) < 0$, because for all experimentally studied molecular liquids two-phase vapor heat capacity C''_{V_2} is greater than two-phase liquid heat capacity C'_{V_2}, i.e., $C''_{V_2} > C'_{V_2}$. Thus, Yang—Yang anomaly strength parameter R_μ should be negative for all liquids (the sign is independent on the molecular structure). The values of Yang—Yang anomaly strength parameter R_μ as a function of temperature calculated from Eq. (15) using the present two-phase isochoric heat capacity data near the critical point for benzene are shown in Fig. 14. As can be seen, R_μ is negatively diverging as the critical temperature approaches. Cerdeiriña et al. [77] studied the Yang—Yang anomaly using a compressible cell gas (CCG) model that obeys complete scaling with pressure mixing. They found that when the discrete local CCG cell volumes

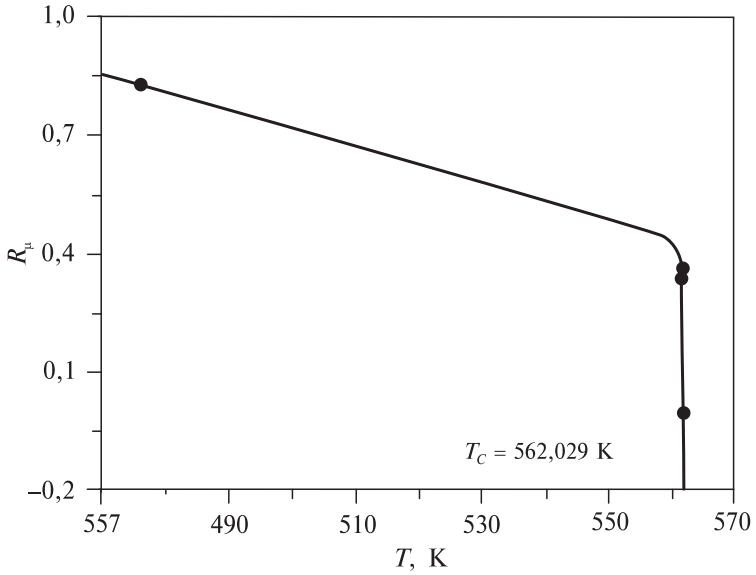

Fig. 14. TheYang–Yang anomaly strength parameter R_μ for benzene as a function of temperature derived from the two-phase isochoric heat capacities (C_{V_2}' and C_{V_2}'') and saturated liquid and vapor specific volume(V' and V'') measurements near the critical point, Eq. (15)

fluctuate freely the Yang—Yang anomaly parameter R_μ may take any values between $-\infty$ and 0,5. Therefore, our calorimetric (two-phase C_{V_2}) measurements near the critical point for benzene clearly confirm the theoretical prediction of Cerdeiriña et al. [77]. However, the value, the physical meaning, the magnitude, or even the sign of the R_μ is still unknown. Therefore, present experimental results can be used to improve and confirm the main physical basis of the complete scaling theory of the critical phenomena.

The value of the Yang—Yang anomaly strength parameter $R_\mu = -0{,}683$ was estimated from the present saturated liquid and vapor density measurements using a direct fitting procedure described above. For all methods of R_μ determination (direct two-phase C_{V_2} measurements, Eq. (15), saturated liquid and vapor density fitting, Eq. 7, 10, and 11) the value of the Yang—Yang anomaly strength parameter for benzene is negative, $R_\mu < 0$, although the absolute value is different. The negative value of R_μ means that the mixing coefficient is negative, $a_3 < 0$, its absolute value is less than 1, $|a_3| < 1$, and that the amplitude of the «complete» scaling term $B_4 < 0$ is also negative, $B_4 = \dfrac{a_3}{1 + a_3} B_0^2 < 0$ (for benzene, $B_4 = -1{,}225$).

It is a problem to accurately estimate the value of the asymmetric parameter a_3 from fitting the saturated liquid and vapor densities to Eq. (7) with the restrictions of Eq. (11), especially when inconsistent caloric C_{V_2} (parameters A_0^- and B_{cr}) and saturated liquid and vapor densities (ρ_S' and ρ_S'') measurements are used. Also, an empirical determination of the fitting parameter strongly depends on the input data, such as the fitting temperature range, statistical weight of the experimental data points, etc. This is a possible reason why the directly calculated values of R_μ from Eq. (15) using C_{V_2} measurements and using the fitting procedure from Eq. (7) are different. It is apparently impossible to get negative infinite value for R_μ using a fitting procedure, although it is clear that the value of the asymmetric parameter a_3 should be negative and very close to 1.

In other words, in an ideal case it should be $a_3 = -1$, therefore, $R_\mu = a_3/(1 + a_3) \to -\infty$ and in good agreement with the direct method of the Yang—Yang parameter estimation from C_{V_2} measurements using Eq. (15). Thus, it is very likely that the asymmetric parameter a_3 is negative and very close to –1. This is in good agreement with recent theoretical predictions by Cerdeiriña et al. [77] ($-\infty < R_\mu < 0{,}5$). However, using a fitting procedure, any values of a_3 can be obtained. Thus, the divergence of C_{V_2} in benzene is caused by the positive divergence of $V_C T\left(d^2P_S/dT^2\right)$ and by the negative divergence of $-T\left(d^2\mu/dT^2\right)$. The negative value of the Yang—Yang anomaly strength parameter R_μ was found previously for CO_2 (–0,35) [76, 80], Ne (–0,018), CH_4 (–0,024), N_2 (–0,018), C_2H_4 (–0,0035) [76], and *tret*-butanol (–0,03) [42]. Numerical Monte Carlo simulation [78, 84] of the hard-core square-well fluid also indicates that R_μ is small and negative (close to zero). Orkoulas et al. [84] estimated the value of the Yang—Yang anomaly strength parameter R_μ for carbon dioxide (–0,35) using the values of $\left(d^2P_S/dT^2\right)$ and $\left(d^2\mu/dT^2\right)$ derived from our previously published two-phase isochoric heat capacity data [92]. It is very important to deeply understand the physical nature of the two-phase isochoric heat capacity singularity at the critical point and to improve the existing theory of «complete» scaling.

Asymptotic Critical Amplitudes of Isochoric Heat Capacity and Liquid—Gas Coexistence Curve of Benzene and Universal Critical Amplitude Ratios

According to the scaling theory of critical phenomena [93, 94], the thermodynamic properties of fluids near the critical point exhibit the same singular asymptotic critical behavior as those of a lattice gas. Scaling theory correctly predicts the experimentally observed asymptotic thermodynamic behavior of fluids near the critical point as an asymptotical scaling power laws with universal critical exponents (α, β, γ, δ, ν) [28, 37, 93, 94] and non-universal (system-dependent) critical amplitudes ($A_0^\pm$, B_0, D_0, Γ_0^+, ξ_0). The universality of the scaling functions leads naturally to the universality of the critical amplitude combinations [20, 95—98]. According to the universality principle of the critical phenomena (universality of the scaling functions), only two amplitudes (A_0^+ and B_0, for example) are necessary to determine all other amplitudes such as (D_0, Γ_0^+, Γ_0^-, ξ_0). The universal amplitude combinations are key factors in the study of phase transitions, critical phenomena, and other related issues and are very important for understanding of the current status of theory and experiment. According to the scaling theory (universality principle), the critical amplitude ratios (A_0^-/Γ_0^+, $A_0^+\Gamma_0^+$, $B_0^2, D_0\Gamma_0^+$, $B_0^{\delta-1}, \Gamma_0^+/\Gamma_0^-$) are universal, depend only on universal critical exponents, and are associated with the universal scaling relations between the critical exponents. The universal critical exponents of the isochoric heat capacity ($\alpha = 0{,}11$) and liquid—gas coexistence curve ($\beta = 0{,}324$) and their non-universal asymptotical critical amplitudes ($A_0^\pm$ and B_0) play important role in the theory of critical phenomena and its practical applications for the development of a scaling-type equation of state. For example, the asymptotic critical amplitudes ($A_0^\pm$ and B_0), together with other critical amplitudes (Γ_0^+, D_0, ξ_0), satisfy the universal relations [20—27]: $\dfrac{A_0^+}{A_0^-} = 0{,}524$ [23, 24], $\dfrac{\alpha A_0^+\Gamma_0^+}{B_0^2} = 0{,}058$ [25, 26],, $D_0\Gamma_0^+, B_0^{\delta-1} = 1{,}69$ [26, 27], and $\xi_0\left(\dfrac{\alpha A_0^+}{\nu_C}\right)^{1/3} = 0{,}266$ [20—22] (see also Table 3). The values of other critical amplitudes,

Table 3

Experimental and theoretical universal critical amplitude ratios

Models	$\alpha A_0^+ \Gamma_0^+ B_0^{-2}$	$D_0 \Gamma_0^+ B_0^{\delta-1}$	A_0^+/A_0^-	Γ_0^+/Γ_0^-
Crossover model	0,052	1,64	0,524	4,96
ε expansion	0,048 [23]	1,67	0,520 ± 0,01 [24]	4,90 [23]
d = 3 field theory [90]	0,0594 ± 0 ,0011	—	0,541 ± 0,014	4,77 ± 0,30
3D Ising model [24]	0,058 ± 0,001	—	0,523 ± 0,009	4,95 ± 0,15
Experiment (this work, for benzene)	0,058	1,69	0,524	—

such as Γ_0^+, ξ_0, and D_0, can be estimated using these universal relations and the present values of the critical amplitudes for heat capacity ($A_0^+ = 3{,}091$) and coexistence curve ($B_0 = 1{,}6714$) for benzene as $\Gamma_0^+ = \dfrac{0{,}058 B_0^2}{\alpha A_0^+} = 0{,}477$ ($\Gamma_0^+ = \bar{\Gamma}_0^+ Z_C = 0{,}139$, where $Z_C = 0{,}2925$), $D_0 = \dfrac{1{,}69}{\Gamma_0^+ B_0^{\delta-1}} = 0{,}491$, and $\xi_0 = 0{,}266(\alpha A_0^+ \nu_C)^{-1/3} = 0{,}16$ mm, where ν_C $N_A \rho_C$ is the molecular volume at the critical point. The values of universal critical amplitude ratios predicted by various theoretical models [25—27, 99] are presented in Table 3 together with the values derived from the present experimental isochoric heat-capacity and coexistence curve data for benzene. As one can see from Table 3, the agreement is good enough. In our earlier publication, Perkins et al. [28] used a generalized corresponding states principle to develop acorrelation of the asymptotic critical amplitudes (A_0^+, B_0) in terms of their dependence on the acentric factor ω as

$$A_0^- = 5{,}58 + 7{,}94\omega \text{ and } B_0 = 1{,}45 + 1{,}21\omega. \tag{16}$$

The values of the asymptotic critical amplitudes (A_0^- and B_0) for benzene predicted from Eq. (16) are $A_0^- = 7{,}255$ and $B_0 = 1{,}705$. The uncertainties of the predicted values of (A_0^- and B_0) are 15 % for A_0^- and 10 % for B_0. These predicted values deviate from the present experimental data within 22 % for A_0^- and 2,0 % for B_0, i.e., they are close to their uncertainties.

Also, the derived critical amplitude of the two-phase isochoric heat capacity (A_0^-), the background parameter $\bar{B}_{cr}$, and the asymmetric parameter a_3 of the coexistence curve can be used to estimate vapor-pressure equation parameters (P_1 and P_3). The curvature of the vapor-pressure line derived from the two-phase isochoric heat-capacity measurements by integrating the Eq. (13) can be expressed by the scaling relation

$$\Delta P_S(T) = P_1 t^{2-\alpha} + P_2 t^{2-\alpha+\Delta} + P_3 t^2, \tag{17}$$

where P_i (i = 1,3) are the adjustable parameters, $\Delta = 0{,}52$ is the universal critical exponent [100, 101]. According to the complete scaling theory, the values of the fitting parameters P_1 and P_3 in the vapor-pressure Eq. (17) are related to the critical amplitude A_0^- and the background parameter $\bar{B}_{cr}$ of the isochoric heat capacity (see Eq. 9), and the asymmetric parameter of the coexistence cure diameter a_3 as [25]

$$P_1 = \frac{A_0^-}{(1+a_3)(2-\alpha)(1-\alpha)}, \; P_3 = \frac{1}{(1+a_3)} - \frac{1}{2} B_{cr}. \tag{18}$$

Thus, the values of the fitting parameters P_1 and P_3 of the vapor-pressure equation can be directly calculated from the asymptotic critical amplitudes (A_0^-, B_{cr}) of heat-capacity and asymmetric parameter a_3 of the coexistence curve singular diameter calculated from the presently measured isochoric heat capacities and saturated densities for benzene. This allows one to develop thermodynamically consistent equations for the vapor pressure, saturated liquid and vapor densities, and two-phase heat capacities, therefore, to calculate other thermodynamic properties.

CONCLUSIONS

A new single- and two-phase isochoric heat capacity data for benzene are experimentally obtained and reported in the present work over the temperature range from 347 to 616 K for 6 liquid and 5 vapor isochores between 265 and 653 $kg \cdot m^{-3}$ at pressures up to 7,5 MPa including the critical and supercritical regions. The values of the second temperature derivatives of the vapor-pressure $\left(d^2P_S/dT^2\right)$ and chemical potential $\left(d^2\mu/dT^2\right)$ were calculated as functions of temperature near the critical point by means of the measured two-phase heat capacity C_{V_2} and saturated specific liquid and vapor volumes. We experimentally determined that both $\left(d^2P_S/dT^2\right)$ and $\left(d^2\mu/dT^2\right)$ show discontinuity at the critical point. The discontinuity of $\left(d^2\mu/dT^2\right)$ at the critical point is in good consistence with the «complete» scaling theory prediction. Also, the measured two-phase heat capacities C_{V_2}, together with experimental temperature derivatives of the vapor-pressure $\left(dP_S/dT\right)$ and the saturated specific volume $\left(dV_S/dT\right)$, were used to calculate other derived properties, such as the saturation heat-capacity C_{sat} near the critical point. The measured values of single- and two-phase C_V along the critical isochore and the liquid+gas coexistence curve densities near the critical point were used to estimate the values of the asymptotic critical amplitudes ($A_0^- = 3{,}091$ and $B_0 = 1{,}671$) and related amplitudes for other properties ($D_0 = 0{,}491$, $\bar{\Gamma}_0 = 0{,}139$, and $\xi_0 = 0{,}16$ nm) using universal relations between the critical amplitudes. Two distinct contributions (vapor- pressure, C_{VP}, and chemical potential, $C_{V\mu}$) to the measured total two-phase C_{V_2} values, using the well-known Yang—Yang relation, were estimated. The derived C_{VP} and $C_{V\mu}$ were then used to estimate the values of the Yang—Yang anomaly strength parameter R_μ as a function of temperature. It was shown that the sign of R_μ for ordinary studied molecular liquids is negative and a strong function of temperature near the critical point, i.e., this parameter sharply changes when the critical temperature is approaching. Based on our experimental calorimetric data (C_{V_2}'', C_{V_2}', V'', V') at saturation, we have shown that the Yang—Yang function $R_\mu(T)$ at the critical point (the Yang—Yang anomaly parameter) for benzene trends to take large negative values (negatively diverges, $R_\mu \to -\infty$), which means that the singularity of C_{V_2} at the critical point is shared between the vapor-pressure C_{VP} and chemical potential $C_{V\mu}$ contributions. The measured saturated liquid and vapor densities were used to calculate the asymmetric parameters a_3 and b_2 of the liquid + gas coexistence curve (singular diameter). The asymmetry coefficient $a_3 = -0{,}152$ and $b_2 = -0{,}6393$ for benzene are negative, meaning that the «complete» scaling contribution is negative $\frac{a_3}{1+a_3} B_0^2 t^{2\beta} < 0$, while the «incomplete» scaling contribution is positive $-b_2 \frac{A_0^-}{(1-\alpha)} t^{1-\alpha} > 0$.

For benzene, the singularity of the coexistence curve diameter ρ_d is shared between the «incomplete» $t^{1-\alpha}$ and «complete» $t^{2\beta}$ terms. We found that for benzene $R_\mu < 0$ (probably $R_\mu \to -\infty$), while $a_3 < 0$ and should be very close to –1. However, the present study has demonstrated that the physical meaning of the Yang—Yang anomaly parameter is still unclear. It is even a problem to correctly estimate its magnitude and sign as was mentioned earlier by $R_\mu \to -\infty$ Cerdeiriña et al. [77].

ACKNOWLEDGMENT

This work was supported by the Russian Foundation of Basic Research (RFBR) grants №19-08-00056 and №18-08-00500.

REFERENCES

1. *Savage P.E., Gopalan S., Mizan T.I., Martino C.J., Brock E.E.* // AIChE J. 1995. Vol. 41. P. 1723.
2. *Karmore V., Madras G.* // Ind. Eng. Chem. Res. 2000. Vol. 39. P. 4020.
3. *Polikhronidi N.G., Abdulagatov I.M., Magee J.W., Batyrova R.G.* // J. Chem. Eng. Data. 2001. Vol. 46. P. 1064.
4. *Polikhronidi N.G., Abdulagatov I.M., Magee J.W., Stepanov G.V.* // Int. J. Thermophys. 2001. Vol. 22. P. 189.
5. *Polikhronidi N.G., Abdulagatov I.M., Magee J.W., Stepanov G.V.* // Int. J. Thermophys. 2002. Vol. 23. P. 745.
6. Polikhronidi *N.G., Abdulagatov I.M., Magee J.W., Stepanov G.V.* // Int. J. Thermophys. 2003. Vol. 24. P. 405.
7. *Polikhronidi N.G., Abdulagatov I.M., Magee J.W., Stepanov G.V., Batyrova R.G.* // Int. J. Thermophys. 2007. Vol. 28. P. 163.
8. *Polikhronidi N.G., Batyrova R.G., Abdulagatov I.M., Magee J.W., Stepanov G.V.* // J. Supercrit. Fluids. 2004. Vol. 33. P. 209.
9. *Polikhronidi N.G., Batyrova R.G.,Abdulagatov I.M., Stepanov G.V.* // Int. J. Thermophys. 2006. Vol. 27. P. 729.
10. *Polikhronidi N.G., Abdulagatov I.M., Stepanov G.V., Batyrova R.G.* // Fluid Phase Equilib. 2007. Vol. 252. P. 33.
11. *Polikhronidi N.G., Abdulagatov I.M., Batyrova R.G., Stepanov G.V.* // Int. J. Thermophys. 2009. Vol. 30. P. 737.
12. *Polikhronidi N.G., Batyrova R.G.,Abdulagatov I.M., Magee J.W.,Wu J.T.* // Phys. Chem. Liq. 2014. Vol. 52. P. 657.
13. *Polikhronidi N.G., Batyrova R.G., Abdulagatov I.M., Magee J.W., Wu J.T.* // Int. J. Thermophys. 2016. Vol. 37. P.103.
14. *Polikhronidi N.G., Abdulagatov I.M., Batyrova R.G., Stepanov G.V.,Wu J.T., Ustuzhanin E.E.* // Int. J. Thermophys. 2012. Vol. 33. P. 185.
15. *Polikhronidi N.G., Abdulagatov I.M., Stepanov G.V., Batyrova R.G.* // J. Supercrit. Fluids. 2007. Vol. 43. P. 1.
16. *Polikhronidi N.G., Abdulagatov I.M., Batyrova R.G.* // Fluid Phase Equilib. 2002. Vol. 201. P. 269.
17. *Polikhronidi N.G., Abdulagatov I.M., Batyrova R.G., Stepanov G.V.* // Int. J. Thermophys. 2009. Vol. 30. P. 737.
18. *Gamidov Sh.G.* // Ph.D. Thesis, Azerbaidjan State University. Baku. 1971.
19. *Chirico R.D., Steele W.V.* // Ind. Eng. Chem. Res. 1994. Vol. 33. P. 157.
20. *Privman V., Hohenberg P.C., Aharony A.* // In: Phase Transitions and Critical Phenomena. Ed. C. Domb, L. Lebowitz, AP, NY, 1999. Vol. 14. P. 367.
21. *Pelissetto A., Vicari E.* // Physics Reports. 2002. Vol. 368. P. 549.
22. *Fisher M.E., Zinn Sh.-Y.* // J. Phys. A: Math. Gen. 1998. Vol. 319. P. L629.
23. *Nicoll F., Albright P.C.* // Phys. Rev. B 1985. Vol. 31. P. 4576.
24. *Bervillier C.* // Phys. Rev. B 1986. Vol. 34. P. 8141.

25. *Behnejad H., Sengers J.V., Anisimov M.A.* / In: Appl. Thermodyn. Fluids. Eds. A.R.H. Goodwin, J.V. Sengers, C.J. Peters, IUPAC. 2010. Chap. 10. P. 321.
26. *Kiselev S.B., Sengers J.V.* // Int. J. Thermophys. 1993. Vol. 14. P. 1.
27. *Kiselev S.B., Kostukova I.G., Povodyrev A.A.* // Int. J. Thermophys. 1991. Vol. 12. P. 877.
28. *Perkins R.A., Sengers J.V., Abdulagatov I.M., Huber M.L.* // Int. J. Thermophys. 2013. Vol. 34. P. 191.
29. *Amirkhanov Kh.I., Stepanov G.V., Abdulagatov I.M., Bui O.A.* // Dagestan Scientific Center of the Russian Academy of Sciences, Makhachkala. 1989.
30. *Abdulagatov I.M., Magee J.W., Polikhronidi N.G., Batyrova R.G.* // In: Enthalpy and Internal Energy: Liquids, Solutions and Vapors. Ed. T. Letcher, E. Wilhelm // Royal Society of Chemistry. 2017. Chap. 15. P. 380.
31. *Amirkhanov Kh.I., Stepanov G.V., Alibekov B.G.* / Isochoric Heat Capacity of Water and Steam. Amerind Publ. Co., New Delhi, NBS, USA Department of Commerce, NSF. 1974.
32. *Wagner W., Pruß A.* // J. Phys. Chem. Ref. Data. 2002. Vol. 31. P. 387.
33. *Mursalov B.A., Abdulagatov I.M., Dvoryanchikov V.I., Kiselev S.B.* // Int. J. Thermophys. 1999. Vol. 20. P. 1497.
34. Giude to the Expression of Uncertainty in Measurement; ISO: Geneva, Switzerland. 1993.
35. *Kim S.H., Kang J.W., Kroenlein K., Magee J.M., Diky V., Muzny Ch., Kazakov A.F., Chirico R.D., Frenkel M.* // Chem. Eng. Ed. 2013. Vol. 47. P. 48.
36. *Polikhronidi N.G., Abdulagatov I.M., Batyrova R.G., Stepanov G.V.* // Int. J. Refrigeration. 2009. Vol. 32. P.1897.
37. *Sengers J.V., Levelt Sengers J.M.H.* // Annual Review Physical Chemistry 1986. Vol. 37. P. 189.
38. *Rowlinson J., Swinton F.L.* Liquids and Liquid Mixtures. 3rd ed. Butterworths, London. 1982.
39. *Polikhronidi N.G., Batyrova R.G., Abdulagatov I.M.* // Fluid Phase Equilib. 2000. Vol. 175. P. 153.
40. *Polikhronidi N.G., Batyrova R.G., Abdulagatov I.M.* // Int. J. Thermophys. 2000. Vol. 21. P. 1073.
41. *Valyashko V.M., Abdulagatov I.M., Levelt- Sengers J.H.M.* // J. Chem. Eng. Data. 2000. Vol. 45. P. 1139.
42. *Radzhabova L.M., Stepanov G.V., Abdulagatov I.M.* // Fluid Phase Equuilib. 2011. Vol. 309. P. 128.
43. *Radzhabova L.M., Stepanov G.V., Abdulagatov I.M., Shakhbanov K.A.* // J. Supercritical Fluids. 2012. Vol. 63. P. 115.
44. *Radzhabova L.M., Stepanov G.V.,Abdulagatov I.M., Shakhbanov K.A.* // Phys. Chem. Liquids. 2012. Vol. 50. P. 1.
45. *Kamilov I.K., Stepanov G.V., Abdulagatov I.M., Rasulov A.R., Milikhina E.M.* // J. Chem. Eng. Data. 2001. Vol. 46. P. 1556.
46. *Bezgomonova E.I., Abdulagatov I.M., Stepanov G.V.* // J. Mol. Liquids. 2012. Vol. 175. P. 12.
47. *Bezgomonova E.I., Abdulagatov I.M., Stepanov G.V.* // J. Mol. Liquids. 2012. Vol. 175. P. 121.
48. *Polikhronidi N.G., Abdulagatov I.M., Batyrova R.G., Stepanov G.V.* // Fluid Phase Equilib. 2010. Vol. 292. P. 48.
49. *Polikhronidi N.G., Batyrova R.G., Abdulagatov I.M., Stepanov G.V., Wu J.T* // J. Chem. Thermodyn. 2012. Vol. 53. P. 67.
50. *Polikhronidi N.G., Stepanov G.V., Abdulagatov I.M., Batyrova R.G.* // Thermochim. Acta. 2007. Vol. 454. P. 99.
51. *Polikhronidi N.G., Abdulagatov I.M., Batyrova R.G., Stepanov G.V.* // Intl. J. Thermophys. 2011. Vol. 32. P. 559.
52. *Lemmon E.W., Huber M.L., McLinden M.O.* / NIST Standard Reference Database 23. NIST Reference Fluid Thermodynamic and Transport Properties, REFPROP, version 9.1. Standard Reference Data Program. National Institute of Standards and Technology, Gaithersburg, MD. 2018.
53. *Yang C.N, Yang C.P.* // Phys. Rev. Lett. 1969. Vol. 13. P. 303.

54. *Abdulagatov A.I., Stepanov G.V., Abdulagatov I.M., Ramazanova A.E., Alisultanova G.A.* // Chem. Eng. Comm. 2003. Vol. 190. P. 1499.
55. *Polikhronidi N.G., Abdulagatov I.M., Batyrova R.G., Stepanov G.V., Wu J.T.* // Int. J. Thermophys. 2012. Vol. 33. P.185.
56. *Gaddy E.M., White J.A.* // Phys. Rev. A 1982. Vol. 26. P. 2218.
57. *Stephenson J.* // Can. J. Phys. 1976. Vol. 54. P. 1282.
58. *Magee J.W., Kaboyashi R.* // In: Proc. 8th Symp. Thermophysical Properties Symp. Vol. 1: Thermophysical Properties of Fluids. Ed. J.V. Sengers. ASME: New York. 1982. P. 321.
59. *Magee J.W.* // The 20th Japan Symp. on Thermophys. Prop. Tokyo. 1999. P. 473.
60. *Magee J.W.* // Int. J. Thermophys. 1996. Vol. 17. P. 803.
61. *Theeuwes F., Bearman R.J.* // J. Chem. Thermodyn. 1970. Vol. 2. P. 513.
62. *Bearman R.J., Theeuwes F., Bearman M.Y., Mandel F., Throop G.J.* // J. Chem. Phys. 1970. Vol. 52. P. 5486.
63. *Diller D.E.* // Cryogenics. 1971. Vol. 6. P. 186.
64. *Gladun C.* // Cryogenics. 1971. Vol. 4. P. 78.
65. *Oliver D., Eaton M., Huffman H.M.* // J. Am. Chem. Soc. 1948. Vol. 70. P. 1502.
66. *Hales J.L., Townsend R.J.* // Chem. Thermodyn. 1972. Vol. 4. P. 763.
67. *Skaates J.M., Kay W.B.* // Eng. Sci. 1964. Vol. 19. P. 431.
68. *Hales J.L., Gundry H.A.* // J. Phys. E. 1983. Vol. 16. P. 91.
69. *Connolly J.F., Kandalic G.A.* // J. Chem. Eng. Data. 1962. Vol. 7. P. 137.
70. *Kooner Z.S., Van Hook W.A.* // J. Phys. Chem. 1986. Vol. 90. P. 4860.
71. *Campbell A.N., Chatterjee R.M.* // Can. J. Chem. 1968. Vol. 46. P. 575.
72. *Artukhovskaya L.M., Shimanskaya E.T., Shimanskii Yu.I.* // Ukr. Fiz. Zh. 1970. Vol. 15. P. 1974.
73. *Akhundov T.S., Abdullaev F.G.* // Izv. Vyssh. Uchebn. Zaved., NefteGaz. 1977. Vol. 7. P. 64.
74. *Gorbunova N.I., Simonov Y.M., Shipova Y.A.* // In: Proceedings of the 8th Symposium on Thermophysical Properties. ASME: New York, 1982. Vol. 2. P. 429.
75. *Straty G.C., Ball M.J., Bruno T.J.* // J. Chem. Eng. Data. 1987. Vol. 32. P. 163.
76. *Fisher M.E., Orkoulas G.* // Phys. Rev. 2000. Vol. 85. P. 696.
77. *Cerdeirina C.A., Orkoulas G., Fisher M.E.* // Phys. Rev. Lett. 2016. Vol. 116. P. 040601.
78. *KimY.C.* // Phys. Rev. E. 2005. Vol. 71. P. 051501-1.
79. *Nicoll J.F.* // Phys. Rev. A. 1981. Vol. 24. P. 2203.
80. *Orkoulas G., Fisher M.E., Ustun C.* // J. Chem. Phys. 2000. Vol. 113. P. 7530.
81. *Rehr J.J., Mermin N.D.* // Phys. Rev. A. 1973. Vol. 8. P. 472.
82. *Mermin N.D.* // Phys. Rev. Lett. 1971. Vol. 26. P.169.
83. *Kim Y.C., Fisher M.E., Orkoulas G.* // Phys. Rev. E . 2003. Vol. 67. P. 061506.
84. *Orkoulas G., Fisher M.E., Panayiotopoulos A.Z.* // Phys. Rev. E. 2001. Vol. 63. P. 051507-1.
85. *Patricia Losada-Perez, Cerdeiriña C.A.* // J. Chem.Thermodyn. 2017. Vol. 109. P. 56.
86. *Anisimov M.A., Wang J.* // Phys. Rev. 2006. Vol. 97. P. 025703-1.
87. *Wang J., Anisimov M.A.* // Phys. Rev. E. 2007. Vol. 75. P. 051107-1.
88. *Lee T.D., Yang C.N.* // Phys. Rev. 1952. Vol. 87. P. 410.
89. *Mermin N.D.* // Phys. Rev. Lett. 1971. Vol. 26. P. 957.
90. *Widom B., Rowlinson J.S.* // J. Chem. Phys. 1970. Vol. 52. P. 1670.
91. *Abdulagatov I.M., Polikhronidi N.G., Batyrova R.G.* // Fluid Phase Equilib. 2016. Vol. 415. P. 144.
92. *Abdulagatov I.M., Polikhronidi N.G., Batyrova R.G.* // J. Chem. Thermodyn. 1994. Vol. 26. P. 1031.
93. *Fisher M.E.* / Critical Phenomena. Lectures Notes in Physics. F.J.W. Hahne ed. Springer: Berlin, 1988. Vol. 186. P. 1.
94. *Fisher M.E.* // Rep. Prog. Phys. 1967. Vol. 30. P. 615.
95. *Barmatz M., Hohenberg P.C., Kornblit A.* // Phys. Rev. B 1975. Vol. 12. P. 1947.
96. *Hohenberg P.C., Aharony A., Halperin B.I., Sigga E.D.* // Phys. Rev. B 1976. Vol. 13. P. 2986.
97. *Stauffer D., Ferer M., Wortis M.* // Phys. Rev. Lett. 1972. Vol. 29. P. 345.
98. *Betts D.D., Guttmann A.J., Joyce G.S.* // J. Phys. C. 1971. Vol. 4. P. 1994.
99. *Bagnuls C., Bervilliev C.* // Phys. Rev. B. 1985. P. 32. P. 7209.
100. *Guida R., Zinn-Justin S.* // J. Phys. A. 1998. Vol. 31. P. 8103.
101. *Saul D.M., Wortis M., Jasnow D.* // Phys. Rev. B 1975. Vol. 11. P. 2571.

КРИТИЧЕСКИЕ И СВЕРХКРИТИЧЕСКИЕ ЯВЛЕНИЯ В БЕНЗОЛЕ

Н.Г. Полихрониди, Р.Г. Батырова, И.М. Абдулагатов

Институт Физики Дагестанского Научного Центра Российской Академии Наук, Махачкала, Дагестан, Российская Федерация
Институт Проблем Геотермии Российской Академии Наук, Махачкала, Дагестан, Российская Федерация
Дагестанский Государственный Университет

Одно- (C_V) и двух- фазные (C_{V_2}) теплоемкости при постоянном объеме, плотность (ρ_S), температура в точке фазового перехода (T_S) бензола были измерены в критической и сверхкритической областях. Измерения были проведены в непосредственно близи температуры фазового перехода жидкость-газ и критической точки, для точного определения термодинамических свойств (T_S, ρ_S, C_{V_1}, C_{V_2}) на кривой сосуществования жидкость-газ. Измерения проводились в температурном интервале от 347 до 616 K для 6 жидких и 5 паровых изохор между 265 и 653 кг · м$^{-3}$ при давлениях до 7,5 МПа, используя высокотемпературный адиабатический калориметр высокого давления. Погрешность измерения плотности, температуры, и изохорной теплоемкости, C_V, с уровнем доверительной вероятности 95 %, составляет 0,15 %, 15 мК, и 3 %, соответственно. Измеренные значения одно- (C_{V_1}) и двух-фазной (C_{V_2}) теплоемкостей вдоль критической изохоры и плотности на линии насыщения со стороны жидкости (ρ_S') и пара (ρ_S'') вблизи критической точки были использованы для точного определения теоретически важных асимптотических критических амплитуд (A_0^+ и B_0) и связанных с ними амплитуд других термодинамических свойств (Γ_0^+, D_0, ξ_0) и их универсальных соотношений, A_0^+/A_0^-, $A_0^+\Gamma_0^+B_0^2$, $\alpha A_0^+\Gamma_0^+B_0^{-2}$, $D_0\Gamma_0^+B_0^{\delta-1}$, $\xi_0\left(\frac{\alpha A_0^+}{\nu_C}\right)^{1/3}$. Плотности на линии насыщения вместе с измеренными значениями двухфазных теплоемкостей C_{V_2}, были использованы для определения значения параметра асимметрии a_3 (параметра теории «завершенного» скейлинга) и параметра b_2 сингулярного диаметра кривой сосуществования. Экспериментально определенные асимптотические критические амплитуды (A_0^+ и B_0, индивидуальные параметры вещества), были использованы для проверки и подтверждения предсказывающей способности универсальных соотношений, описывающих зависимость критических амплитуд от ацентрического фактора ω, на основе обобщенного принципа соответственных состояний. Измеренные значения C_{V_2} как функция удельного объема V вдоль различных изотерм в двухфазной области были использованы для определения температурных производных давления насыщенных паров $\frac{d^2P_S}{dT^2}$ и химического потенциала $\frac{d^2\mu}{dT^2}$, и оценки параметра Янг—Янг аномалии R_μ для бензола. Вклад давления насыщенных паров, $C_{VP} = V_C T\frac{d^2P_S}{dT^2}$, и химического потенциала, $C_{V\mu} = -T\frac{d^2\mu}{dT^2}$, в сингулярность экспериментально наблюдаемое значение полной двухфазной теплоемкости $C_{V_2} = C_{V\mu} + C_{VP}$ были определены.

Ключевые слова: адиабатический калориметр; бензол; параметр асимметрии, критические амплитуды; критическая точка; изохорная теплоемкость; параметр Янг—Янг аномалии.